SEDIMENT DISPERSAL, RESERVOIR QUALITY, AND PROVENANCE ANALYSIS OF THE EARLY MISSOURIAN CLEVELAND SANDSTONE, WESTERN ANADARKO BASIN, OKLAHOMA

By

BRANDON M. WEAVER

Bachelor of Science in Geology

Texas Christian University

Fort Worth, Texas

2020

Submitted to the Faculty of the
Graduate College of the
Oklahoma State University
in partial fulfillment of
the requirements for
the Degree of
MASTER OF SCIENCE
May, 2022

SEDIMENT DISPERSAL, RESERVOIR QUALITY, AND PROVENANCE ANALYSIS OF THE EARLY MISSOURIAN CLEVELAND SANDSTONE, WESTERN ANADARKO BASIN, OKLAHOMA

Thesis Approved:

Dr. James Puckette

Thesis Adviser

Dr. Jack Pashin

Dr. Mary Hileman

Dr. James Knapp

ACKNOWLEDGEMENTS

I would like to thank my advisor, Dr. Jim Puckette, for his role in developing me into a better scientist and professional. Most of all, I thank him for his positive attitude and his unwavering confidence in myself and this study. My committee members, Drs. James Knapp, Jack Pashin, and Mary Hileman deserve the same praise; I thank you all for your dedication to the Boone Pickens School of Geology and its students. This project could not have been completed without Keith Edmonds, the benefactor of this study. Thank you, Mr. Edmonds, for giving students such as myself the opportunity to advance our education in the geosciences; your contributions are more valuable than you know, and certainly do not go unappreciated.

Several other individuals and institutions contributed greatly to this study. The Oklahoma Petroleum Information Center (OPIC), and specifically Vyetta Jordan, provided invaluable data to the project, including photomicrographs, core data, RCA data, and well log data. My colleague and fellow graduate student, Dylan Morton, was never too busy to brainstorm or answer a trivial question. The Arizona LaserChron Center analyzed detrital zircon samples and provided useful software and documentation to aid in interpretation.

Finally, I would like to thank my family: my father, Troy, my mother, Leslie, and my brother, Carson. Without you guys…well, life would be no fun. I love you all very much, and dedicate the work herein to you.

Name: BRANDON M. WEAVER

Date of Degree: MAY, 2022

Title of Study: SEDIMENT DISPERSAL, RESERVOIR QUALITY, AND PROVENANCE ANALYSIS OF THE EARLY MISSOURIAN CLEVELAND SANDSTONE, WESTERN ANADARKO BASIN, OKLAHOMA

Major Field: GEOLOGY

Abstract: Distribution of Late Paleozoic strata in the Anadarko basin was driven by a complex interplay between the tectonic activity of several potential source areas, cyclic flooding of the North American Craton due to Gondwanan glaciation driven by Milankovitch cycles, and basin physiography. During the early Missourian, the Cleveland Sandstone was being deposited in the western Anadarko basin as well as on the Cherokee platform in central and eastern Oklahoma via fluvial systems; petrographic work performed in this study reveals key differences in the formation between the two areas which may indicate a change in provenance. The Cleveland Sandstone as it occurs in the study area contains abundant low-grade metamorphic rock fragments, where dissolution of these grains creates the majority of porosity in this important hydrocarbon reservoir. This study reports 270 concordant detrital zircon U-Pb ages and 27 new εHf(t) values for the one Cleveland sample analyzed; this is the first reported geochronologic data for the formation. Incorporation of petrographic work with detrital zircon geochronology allows for a greater understanding of sediment dispersal and provenance of this tight sandstone reservoir, which remains poorly understood.

Zircons in the sample analyzed are characterized by an abundance of ages corresponding to the Grenville province (1300-950 Ma), with significant amounts of grains also corresponding to Middle Paleozoic sources (490-270 Ma), Neoproterozoic sources (790-530 Ma), and the Granite-Rhyolite province (1600-1300 Ma). Comparative analysis of published detrital zircon ages and εHf(t) values from Late Paleozoic strata in several different basins, as well as from basement rocks across the North American Craton, reveal that the Cleveland Sandstone was likely sourced primarily from distal extrabasinal systems rather than local source areas; these are likely Gondwanan terranes accreted along the Ouachita-Marathon thrust belt to the south, namely the Yucatan, Maya, and Coahuila blocks. Petrographic work supports previous interpretations of a west-east trending incised fluvial valley that deposited the Cleveland Sandstone as it occurs in the study area. These findings have broader implications on Late Pennsylvanian sediment dispersal in the Anadarko basin, as the presence of these southerly-derived grains have only recently been documented in published literature.

TABLE OF CONTENTS

Chapter Page

LIST OF TABLES

LIST OF FIGURES

Figure Page

Figure Page

CHAPTER I

INTRODUCTION

Petrographic differences in the Cleveland Sandstone across Texas and Oklahoma indicate spatial variability in rock composition and fabric. Consideration of these differences with new insights from detrital zircon geochronologic data sheds light on sediment dispersal and provenance of this tight sandstone reservoir, which is currently poorly understood. This study presents 270 concordant U-Pb detrital zircon ages and 27 Hf ages analyzed from one Cleveland Sandstone well in the western Anadarko basin; these ages are the first published geochronologic data for the formation. Thin section petrography for several wells in the study area was performed to characterize detrital constituents and porosity development, and a paragenetic sequence was created to describe diagenetic events observed in thin sections.

Previous petrographic studies of the Cleveland Sandstone as it occurs in the Texas Panhandle and western Oklahoma indicate abundant low-grade metamorphic rock fragments, with porosity primarily in the form of dissolved metastable grains (Hentz, 1992). Petrographic work from this study, as well as Hentz (1992), Bacon (2012), and Cain (2017) allows for comparison of the formation's composition across the Anadarko basin and Cherokee platform; insights gained from this comparative petrography, along with new geochronologic data, help to delineate sediment dispersal and provenance, and may indicate a change in source from the Cleveland Sandstone in the deep Anadarko basin versus its counterpart on the Cherokee platform.

Former interpretations of the formation's provenance include sourcing from the adjacent Wichita uplift and Ancestral Rocky Mountains (Hentz, 1992). After the discovery of U-Pb zircon ages indicative of Appalachian-derived detritus from Pennsylvanian strata in the Grand Canyon, many recent provenance studies have found further evidence of a northeast-southwest transcontinental fluvial system delivering Appalachian detritus across the North American Craton (Gehrels, 2011; Thomas, 2017; Chapman and Laskowski, 2019). The presence of these grains within the Cleveland Sandstone would greatly affect our current understanding of the formation's depositional history and would have broader implications for Pennsylvanian sediment dispersal in the Anadarko basin. Likewise, relative abundance of other age groups provides a crucial framework for sediment dispersal models, which in turn helps to predict spatial and temporal variability in rock composition and associated reservoir quality.

CHAPTER II

REVIEW OF LITERATURE

2.1 Previous Studies

The majority of research over the Cleveland Sandstone focuses on the formation in north-central and northeastern Oklahoma, where it has produced oil and gas since 1904 (Campbell, 1997). Early researchers such as Baker (1958), Cary (1955), and Clare (1963) described the Cleveland Sandstone as a fine- to coarse-grained calcareous and micaceous sandstone with occasional glauconite and green shale fragments. The Ouachita uplift is widely accepted to be the source of sediment for the easterly-sourced Cleveland Sandstone in north-central and north-eastern Oklahoma (Rascoe and Adler, 1983). However, the abundance of micas within the Cleveland Sandstone led Campbell (1997) to propose an additional granitic source, which he believed to be the Ozark uplift. Kousparis (1979) created contour maps in part of Logan County, Oklahoma on petrophysical characteristics computed from subsurface electrical data. Rottman (1997) studied local geology at the Pleasant Mound oil field and characterized the Cleveland Sandstone reservoir through electric log correlation and core analysis.

Bacon (2012) interpreted the Cleveland Sandstone within a sequence-stratigraphic framework, used thin-section petrography and core observations to characterize reservoir properties, and mapped sediment dispersal patterns in north-central Oklahoma. He also identifies the Nuyaka Creek Shale as separating the “true” Cleveland Sandstone above from Marmaton

Group siliciclastics below. Samples from Bacon (2012) were primarily classified as sublitharenites, with two samples plotting as quartzarenites and one sample plotting as a subarkose on a QRF diagram (Folk, 1968). These samples contained few feldspars, but showed an abundance of lithic fragments, primarily chert.

Cain (2017) studied the Cleveland Sandstone in outcrop and mapped the Kiefer and Owasso sandstone complexes in north-central and northeastern Oklahoma. Through outcrop and core analysis, eight lithotypes were identified based on sedimentary structures, bedding, and lithologies found. Analysis was done with the goal of characterizing the Cleveland Field Unit and like Bacon (2012) placed importance on the Nuyaka Creek Shale in differentiating the true Cleveland Sandstone from underlying Marmaton Group siliciclastics.

More recently, research has focused on identifying bypassed pay zones in mature fields throughout north-central and northeastern Oklahoma. Lupo (2016) utilized high-resolution 3D seismic data to create seismic facies models and map complexly distributed reservoirs. Roddy (2018) evaluated the Cleveland Field in northeastern Oklahoma, divided the Cleveland Sandstone into four units, and calculated petrophysical parameters (water saturation, shale volume, and effective porosity) to further characterize the Cleveland Sandstone reservoir.

Studies of the Cleveland Sandstone in the Texas Panhandle and western Oklahoma are relatively few compared with those in north-central and northeastern Oklahoma. Hentz (1992) gives lithologic descriptions, presents porosity and permeability data, interprets facies and depositional environment through well log interpretation and core observation, and interprets the formation within a sequence-stratigraphic framework in the Texas Panhandle. This was the first regional stratigraphic and sedimentological study of the Cleveland Sandstone in the Texas Panhandle region. Through subsurface mapping, the study identified three distinct parallel, arcuate, north-south trending belts in Cleveland Sandstone distribution throughout Ochiltree,

Lipscomb, Hemphill, Wheeler, Hansford, and Hutchison Counties in northern Texas. These trends were interpreted as stacked delta-front facies occurring at stabilized shoreline positions. A fourth trend, oriented east-west, was interpreted as a fluvial valley incised after a drop in regional base level (Hentz, 1992).

Facies and depositional environment interpretations in Hentz (1992) were accomplished through well log analysis, lithologic descriptions from drilling reports, and analysis of three cores located in Ochiltree and Lipscomb Counties. Hentz (1992) described the Cleveland Sandstone as being white to light gray in color with very fine to fine grains that are subangular to angular. Abundant shale laminae, shale interbeds, and shale lenses were observed, along with massive bedding and cross-lamination. Other descriptors used by Hentz include slightly calcareous, micaceous, and oil stained. Quantitative petrographic analysis of samples obtained from the aforementioned cores was performed to characterize the Cleveland Sandstone, classifying the formation as lithic arkoses and feldspathic litharenites with an average QRF value of $Q_{59}F_{21}R_{20}$ (Hentz, 1992). Unlike the samples analyzed by Bacon (2012), rock fragments observed in Hentz (1992) were primarily low-rank metamorphic rock fragments and plutonic rock fragments; chert was absent or only a minor constituent.

Hentz (1994) discusses the sequence stratigraphy of the Cleveland Formation in the Texas Panhandle as well as basin physiography affecting distribution of facies. Hentz (2011) interprets the Cleveland Sandstone and associated Marmaton siliciclastics in the Texas Panhandle as well as Ellis County, Oklahoma using a refined sequence-stratigraphic framework with seven sequences representing tidally-influenced delta deposits and an incised fluvial valley. Finally, Hentz (2015) studies tidal deposits for Pennsylvanian strata in the Texas Panhandle, including the Cleveland Sandstone.

2.2 Provenance and New Insights into Potential Appalachian Sources

Analysis of sandstone petrography provides unique information related to the provenance of detrital grains (Thomas, 2011). Quantitative methods, such as the QRF ternary diagram created by Folk (1968), led to insights into the tectonic setting of the sediment source as described by Dickinson (1983). More recently, much research has focused on the use of geochronologic data, primarily obtained through U-Pb and Hf detrital zircon analysis, to determine provenance of clastic strata. From these analyses, reconstruction of sediment dispersal relies on incorporating geochronologic data with the stratigraphic, sedimentologic, tectonic, and paleogeographic framework of the sedimentary basin. Often, insights into provenance gained from detrital zircon analyses require adjustments or even total overhauls to these frameworks.

Recently, a study by Gehrels et al. (2011) found that a significant number of detrital zircon dates for Paleozoic sandstones in the Grand Canyon corresponded to ages associated with the Appalachian orogenies. This discovery led to the proposition of a north-east to south-west sediment dispersal system spanning across the North American Craton, necessitating a major change in the paleogeographic frameworks of several North American basins. Many studies, this one included, have since tested this hypothesis (Thomas, 2011; Kissock, 2018; Chapman and Laskowski, 2019; Thomas, 2020; Thomas, 2021).

Prior to Gehrels et al. (2011), studies by Thomas et al. (2004) and Becker et al. (2005) analyze detrital zircon data in the Appalachian basin to identify major sediment contributors from the Alleghanian orogeny. Of the possible components of this orogeny, age signatures from the previous Acadian and Taconic orogenies (490-350 Ma), Grenville province (1200-1000 Ma), and pre-Grenville rocks were dominant in the Pennsylvanian sandstones analyzed. This led Becker et al. (2005) to conclude that Laurentian crust was the main source of sediment to adjacent areas during the Alleghenian orogeny. Thomas (2004) notes that the absence of Alleghenian-aged

samples in synorogenic Appalachian clastic wedge sandstones indicates that these rocks actually contain zircons from the previous Acadian and Taconic orogenies. In other words, Alleghanian igneous rocks had not yet been integrated into the drainage system and/or had not been exhumed, leading to the absence of zircons from this time in synorogenic detritus of areas adjacent to the Alleghanian orogeny.

After the discovery of Appalachian zircons in the Grand Canyon, several studies since have examined detrital zircons in various basins throughout the midcontinent and eastern United States in search of this Alleghanian influence (Kissock, 2018; Chapman and Laskowski, 2019; Thomas, 2020; Thomas, 2021). Kissock (2018) analyzes detrital zircon data for Lower to Middle Pennsylvanian sandstones in the Forest City and Illinois basins in the midcontinent. Their findings suggest a change in provenance from reworked underlying Mississippian strata transported by regional-scale fluvial systems to Appalachian sources (Grenville and Acadian/Taconic orogenic age signatures) transported by extensive extrabasinal fluvial systems. This change in provenance was noted to occur by the Middle Desmoinesian (Kissock, 2018). Three type signatures were identified in detrital zircon ages: (1) a Type 1 detrital zircon signature characterized by a dominance of Midcontinent population ages (1750-1300 Ma), a minimal Neoproterozoic (750-530 Ma) population, and minor to moderate amounts of Superior (>2500 Ma) and Appalachian (490-270 Ma) populations, inferred to be derived from underlying Mississippian strata; (2) a Type 2 detrital zircon signature characterized by the dominance of Appalachian and late Neoproterozoic ages, with minor to moderate Midcontinent grains, possibly derived from the Pan-African terranes associated with Gondwana; and (3) a Type 3 detrital zircon age signature characterized by prominent Appalachian and Midcontinent populations but lacking pre-Granite Rhyolite grains (>1500 Ma), which most resembles coeval strata ages of the central Appalachian foreland basin. Kissock (2018) also links these distinct detrital zircon type signatures to sandstone composition, with Type 1 sandstones being predominantly quartzarenites

and Type 2 and 3 sandstones classifying as subarkoses, sublitharenites, lithic arkoses and feldspathic litharenites with abundant (~5-10%) micas with feldspars and lithic grains.

Chapman and Laskowski (2019) combine over 37,000 U-Pb detrital zircon ages (186 samples) for Ordovician through Pennsylvanian strata in southern Canada, northern Mexico, and the United States (Figure 1). Their study confirms a significant change in provenance for strata across North America beginning in the Mississippian, with zircon age distributions from the Grenville province and Paleozoic grains from the Appalachian forelands extending even to Arizona and California. By Pennsylvanian time, regression of the Kaskaskia sea caused Appalachian-derived detritus to become widespread across North America, likely due to fluvial, deltaic, and aeolian processes (Chapman and Laskowski, 2019). Tunin (2020) compiles 7,845 detrital zircon ages from fifteen studies to characterize potential source provinces for Pennsylvanian strata in the Anadarko basin. Thomas (2021) analyzes detrital zircon data from Mississippian to Permian sandstones in the Fort Worth, Anadarko, and Arkoma basins, concluding that the Arkoma basin marks the southwestward limit of dispersal through the Appalachian foreland, with provenance of the Fort Worth and Anadarko basins being dominated by sediment from Gondwanan terranes accreted in the Ouachita-Marathon foreland.

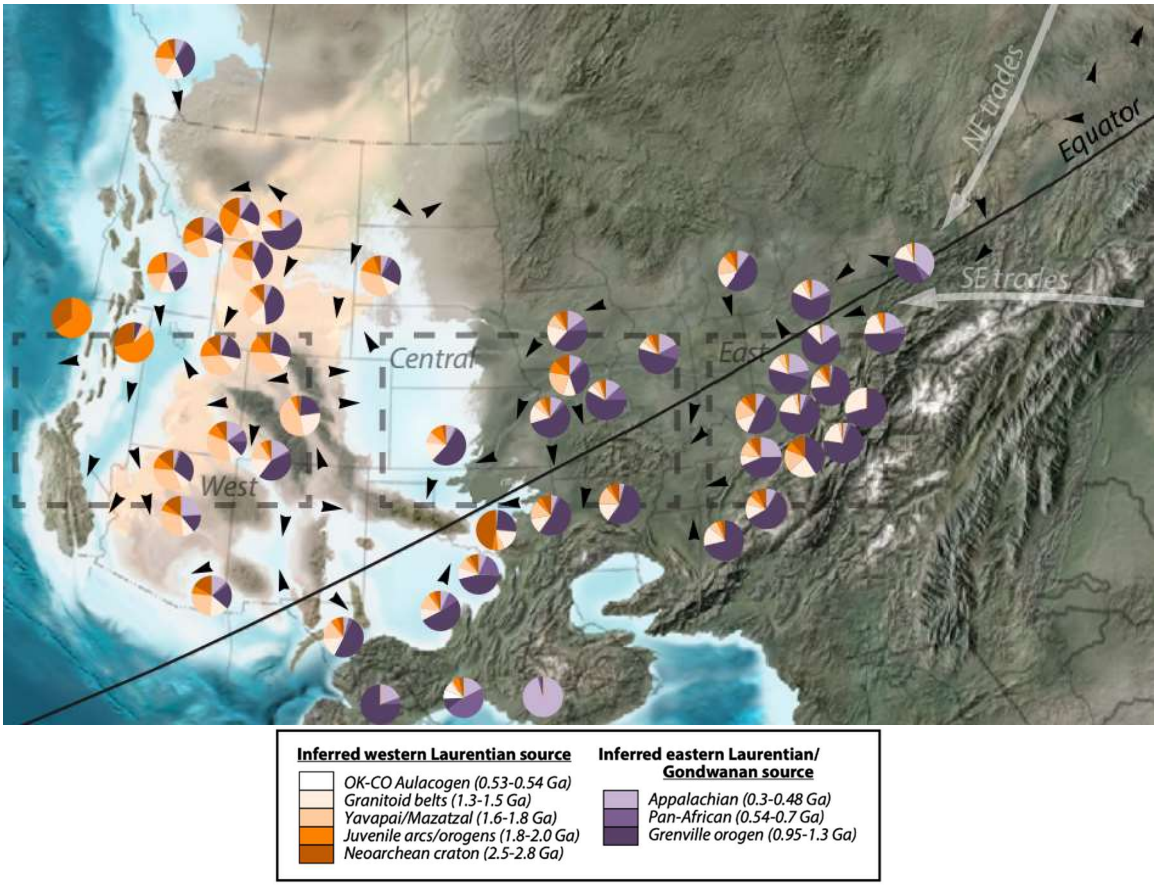

Figure 1. Compiled detrital zircon age distributions plotted as pie diagrams on a Late Pennsylvanian paleogeographic map. Modified from Chapman and Laskowski (2019).

CHAPTER III

GEOLOGIC BACKGROUND

3.1 Pennsylvanian Paleogeography

Distribution of Pennsylvanian strata across North America was driven primarily by the complex tectonic evolution of the craton during the assembly of Pangaea as well as climatic changes associated with Gondwanan glaciation (Johnson, 1989; Algeo, 2008; Miall, 2008; Kissock, 2018). These deposits have a cyclic nature as the low-relief craton was repeatedly flooded by high-frequency glacioeustatic sea-level events (Ross and Ross, 1987b; Miall, 2008; Belt et al., 2011). The major events responsible for constructing the paleogeography of Pennsylvanian strata in the southern midcontinent are: (1) development of sediment sources; (2) closure of the Ouachita embayment; (3) development of the Anadarko basin; and (4) flooding of the craton by the Late Pennsylvanian Midcontinent Sea at the onset of the Absaroka sequence (Sloss, 1963; Moore, 1979; Rascoe and Adler, 1983; Johnson, 1989; Algeo, 2008; Tunin, 2020).

During the Pennsylvanian, North America was undergoing orogenic collision on three of its four margins (Miall, 2008). The collision of Gondwana with the southern and eastern margins of North America caused the Marathon-Ouachita orogeny and the Alleghanian orogeny, while to the west collision with Gondwana resulted in the development of the Ancestral Rockies. These orogenic events resulted in the uplift of several potential sediment sources (Figure 2) for the

midcontinent during the Late Paleozoic (Rascoe and Adler, 1983; Johnson, 1989). The Amarillo-Wichita uplift formed when continental collision during the Early Pennsylvanian resulted in WNW-trending reverse faults that segmented the older southern Oklahoma aulacogen into the strongly positive Amarillo-Wichita uplift and the strongly negative Anadarko and Arkoma basins (Rascoe and Adler, 1983; Johnson, 1989). Thick wedges of clastic sediment, referred to as "granite wash", were eroded from this uplift and deposited in the rapidly subsiding adjacent Anadarko basin. The Cimarron arch, which forms the western margin of the Anadarko basin, and the Nemaha uplift in central Oklahoma and Kansas were likely formed near the end of this tectonic activity, being approximately Atokan in age (Rascoe and Adler, 1983; Johnson, 1989; Hentz, 1992). Until the Early Missourian, the Nemaha uplift separated the deeper Anadarko basin to the west (where the study area of this project is located) from the Cherokee platform and northeastern shelf of the Anadarko basin to the east, inhibiting westward migration of sediment from eastern sources (Moore, 1979). These sources include the Ozark uplift contributing granitic material (Campbell, 1997), the Ouachita Arbuckle uplift contributing siliciclastic sediment (Hentz, 1992), and sediment derived from the Alleghanian orogeny as discussed in section **2.2**. Finally, fine-grained arkosic sediment from the Ancestral Rockies (namely, the Sierra Grande and Apishapa uplifts) was likely shed into the western part of the Anadarko basin throughout the Pennsylvanian (Rascoe and Adler, 1983; Johnson, 1989). Distribution of Pennsylvanian depositional facies in the Anadarko basin is a result of the complex interplay of rapid subsidence and sediment influx from multiple source areas.

In addition to tectonic influences, climate had a significant overprint on Pennsylvanian sediments and depositional systems, with the most significant climatic factor being Gondwanan glaciation driven primarily by ~400,000 year Milankovitch eccentricity cycles (Schutter and Heckel, 1985; Ross and Ross, 1987b; Algeo, 2008). Other factors affecting glaciation and climate

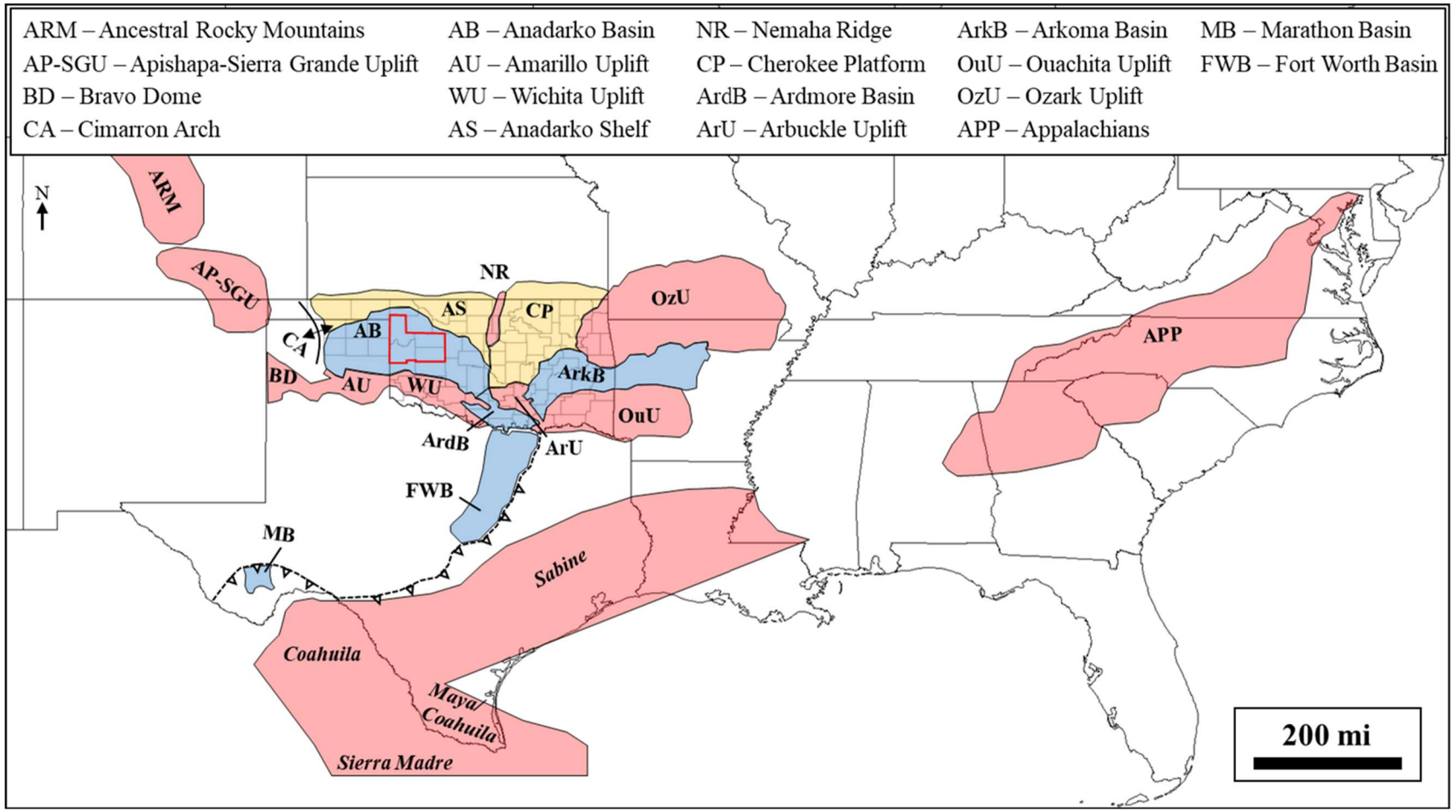

Figure 2. Major tectonic features active during the early Missourian Period. Red polygons indicate structurally positive features, blue polygons indicate structurally negative features, and yellow polygons indicate shelfal areas. Red outline indicates the study area. Compiled from Morris (1974), Moore (1979), Hentz (1992), Becker (2005), Johnson (2008), Miall (2008), and Thomas (2011).

during the Pennsylvanian include changes in geographic position of landmasses, orogenic events, climatic rainfall cycles, flow of ocean surface currents, and general climatic cooling (Ross and Ross, 1987b). These climatic effects can be observed in the Pennsylvanian cyclothems present in the midcontinent, which are comprised of marine limestones with thin shale members and nearshore to terrestrial shales with sandstones and coals (Schutter and Heckel, 1985; Miall, 2008). The abrupt decrease in coals beginning in the Missourian Series as well as the presence of Permian evaporites indicates an overall "drying" trend in the midcontinent from the Mississippian to Permian as North America drifted north away from the equator (Schutter and Heckel, 1985; Algeo, 2008). Largely due to detrital zircon studies of North American basins as discussed in section **2.2**, it is believed that streams and rivers on the North American craton flowed westward during the late Paleozoic (Gehrels et al., 2011; Chapman and Laskowski, 2019).

3.2 Stratigraphy and Depositional Context

Prior to Hentz (1992), no published formal or informal definition of the Cleveland Sandstone existed for the formation in the subsurface Anadarko basin. Since the formation first produced oil in July 1904, the petroleum industry has given the informal subsurface term "Cleveland sand" to various sandstone intervals occurring between the overlying Checkerboard Limestone and the underlying Big Lime/Oswego Limestone (Campbell, 1997; Bacon, 2012; Cain, 2017). Additional marker beds, such as the Dawson coal and Lake Neosho Shale, are also used in correlating the Cleveland sand interval; however, these correlations typically disregard Cleveland stratigraphy as defined at the type outcrop. The "true" Cleveland Sandstone, as defined at this outcrop, lies above the Nuyaka Creek Shale, which represents an interval of rapid transgression and maximum flooding across much of Oklahoma (Hentz, 2011; Bacon, 2012; Cain, 2017). This surface separates the Cleveland Sandstone above from sandstones of the underlying Marmaton Group, and is also the boundary between the Desmoinesian and Missourian Stages (Figure 3) as

defined biostratigraphically by Heckel (1991). The top of the Cleveland Formation is informally defined as the Checkerboard Limestone for the formation in north-central Oklahoma, while in the

Middle Pennsylvanian Stratigraphic Column

System	Sub-system	Series	Group	Anadarko Basin, Western Oklahoma
CARBONIFEROUS	Pennsylvanian	Missourian	Skiatook	Marchand Sand
				Checkerboard LS
				Cleveland Sandstone
				Hepler Sandstone
		Desmoinesian	Marmaton	Lenepah Limestone
				"Wayside" Sand
				Big Lime
				Peru Sand
				Oswego Limestone
			Cherokee	Prue Sand
				Red Fork Sandstone
				Bartlesville Sandstone
				Booch Sand

Figure 3. Stratigraphic column of Middle Pennsylvanian formation in the western Anadarko basin.

Texas Panhandle region the upper boundary is the lowest of five radioactive shale marker beds within the overlying Kansas City Formation (Hentz, 1992; Campbell, 1997). In areas where these marker beds do not display a distinctive gamma-ray signature, correlation of the Cleveland Sandstone proves difficult, contributing to the confusing nomenclature caused by assigning the name "Cleveland" to sandstone units occurring within the Marmaton to Checkboard interval. Additionally, no outcrops of the Cleveland Sandstone exist for the formation in the Texas

Panhandle region, further complicating the stratigraphic framework for the formation in the deep Anadarko basin.

During Morrowan time the Pennsylvanian sea reached its maximum regression and was beginning to transgress upon the recently established structural features of the midcontinent, which were already affecting deposition of Morrowan facies (Moore, 1979). Several shallow-marine and shoreline sands were deposited along the northeastern margin of the Anadarko basin, while deltas supplying sediment from the northwest deposited mostly mud in the northwestern and deep portion of the basin that was subsequently incised by higher-frequency valleys where coarser-grained sediments were trapped mostly during transgression (Rascoe and Adler, 1983; Johnson, 1989; Puckette et al., 2008). The Cherokee platform, also known as the Cherokee reef, was forming during this time as well (Moore, 1979). By the beginning of the Atokan Stage, the major tectonic features of the Pennsylvanian midcontinent had formed, though movement of these features continued intermittently into the Permian (Moore, 1979). The Amarillo-Wichita uplift had been eroded to its granitic basement and was beginning to contribute granite wash clastics to the rapidly subsiding Anadarko basin, with additional sediments entering the basin from the west and northwest (Moore, 1979; Rascoe and Adler, 1983; Johnson, 1989). Atokan strata consist of southward-thickening marine shales, sandstones, and limestones, which grade into massive clastic deposits near the Amarillo-Wichita uplift that consist of igneous- and carbonate-rock fragments (Johnson, 1989). During the early Desmoinesian, much of the midcontinent was periodically inundated; these strata reflect marine conditions alternated with deltaic advances prograding southward across the Cherokee platform and Nemaha ridge (Moore, 1979; Rascoe and Adler, 1983). Deltaic deposition had mostly ceased during the late Desmoinesian, and the southern midcontinent became a broad carbonate shelf (Moore, 1979; Rascoe and Adler, 1983). During the early Missourian, sediments from the Ouachitas had filled

the Arkoma basin, buried the carbonates on the Cherokee platform, and were beginning to spill westward across the Nemaha ridge into the deeper Anadarko basin (Moore, 1979).

In the Texas Panhandle, mapping of the Cleveland Sandstone suggests a western source of siliciclastics, with rock composition (abundant metamorphic and nongranitic plutonic rock fragments and plagioclase framework grains) pointing to nongranitic terranes near the western end of the Anadarko basin as the source of these sediments (Hentz, 1992). This would reflect a change in source from siliciclastics of the underlying Marmaton Group, where mapping and sandstone petrography suggest deltaic deposition from the east (Hentz, 1992; Hentz, 1994; Hentz, 2010; Hentz, 2011; Hentz, 2015). Hentz (1992) proposes the Ouachita foldbelt to the southeast as the source of these Marmaton delta-derived sediments while also acknowledging that additional sources, such as the Sierra Grande-Apishapa uplift to the northwest and the Amarillo-Wichita uplift to the south-southwest, likely contributed sediment as well. Sedimentary structures in Marmaton and Cleveland siliciclastic intervals include asymmetric, double-draped ripples, reactivation surfaces, flaser bedding, rhythmic, laminar stratification (rhythmites), upper flow regime planar stratification, and herringbone stratification; these features along with sandstone body geometry and well log analysis led Hentz (2010, 2011, 2015) to identify these as tidally-influenced delta deposits.

CHAPTER IV

POTENTIAL SEDIMENT SOURCES

The North American Craton offers among the most robust geologic, geophysical, and isotopic data sets of any continent (Whitmeyer, 2007). Detrital zircon analyses require a detailed knowledge of the age, isotopic signature, and sedimentological makeup of potential source terranes for "source to sink" reconstructions. The major source provinces for Paleozoic strata on the North American Craton were formed over billions of years through a series of microcontinental collisions; these are the Superior, Wyoming, Trans-Hudson, Yavapai-Mazatzal, Midcontinent Granite-Rhyolite, Gondwanan-Pan-African accretions, Synrift Igneous, Grenville, and Appalachian synorogenic provinces (Hoffman, 1988; Whitmeyer, 2007; Gehrels et al., 2011; Tunin, 2020). What follows is a discussion on these source provinces organized by geography along with their representative detrital zircon U-Pb isotopic signatures.

4.1 Northern Sources

The northern portion of the North American Craton is occupied by the Canadian Shield, which consists of the Superior (3,500-2,700 Ma), Wyoming (2,700-2,500 Ma), Trans-Hudson (2,300-1,800 Ma), and Grenville (1,300-950 Ma) provinces (Whitmeyer and Karlstrom, 2007; Miall, 2008; Chapman and Laskowski, 2019). Like most other basement provinces on the craton, stratal termination patterns indicate that a significant portion of the Canadian Shield was covered

by sedimentary rocks beginning in the Ordovician and continuing to present day, eliminating the Shield's magmatic and metasedimentary rocks as a readily available sediment source for Pennsylvanian sedimentary rocks (Hoffman, 1988; Miall, 2008; Tunin, 2020). Zircons derived from the Grenville (1,300-950 Ma) province are notorious for their abundance in sedimentary rocks across the North American Craton, and rarely represent first-cycle weathering from the Grenville orogen (Konstantinou, 2013; Chapman and Laskowski, 2019).

4.2 Midcontinent Sources

Several basement exposures were present in the midcontinent during the Pennsylvanian that could have provided proximal detritus to the Anadarko basin. The Nemaha uplift in central Oklahoma and Kansas exposed Precambrian crystalline basement, which included metamorphic, plutonic, and volcanic rocks ranging from 1,700-1,400 Ma, until transgression during the Early Missourian contemporaneous with Cleveland Sandstone deposition covered this uplift (Moore, 1979; Rascoe and Adler, 1983; Johnson, 1989; Whitmeyer, 2007). The Ozark uplift further east exposed similar age rocks derived from pre-Iapetan Precambrian basement through Mississippian passive-margin cover. Rocks with ages 1480-1460 Ma, corresponding to the Eastern Granite-Rhyolite province, are exposed in the St. Francois Mountains in southeastern Missouri at the crest of the Ozark dome and include tuff, rhyolitic flows, granitic plutons, basaltic dikes, and minor inclusions of metamorphic rocks (Thomas, 2012). The Arbuckle uplift in southern Oklahoma exposes rocks of the Southern Granite-Rhyolite province, with granites and gneisses with ages from 1390-1320 Ma (Thomas, 2012; Thomas, 2016). To the south, exposures along the Ouachita foldbelt display a wide range of ages; McGuire (2017) summarizes the ages as roughly 50% Grenville aged grains, 25% Granite-Rhyolite grains, and 25% <950 Ma and Superior aged grains. Cambrian syn-rift igneous rocks with ages 535 ± 10 Ma, associated with late stage rifting of

southeastern Laurentia, also produce zircons common in many North American midcontinent sandstones (Thomas, 2016). These rocks include gabbro, basalt, granite, and rhyolite with strongly positive εHft values, indicating juvenile magmas (Thomas, 2017).

4.3 Western Sources

Recent studies proposing a large transcontinental sediment dispersal system from the Appalachians infer that western sources during the Pennsylvanian would not have contributed a significant amount of sediment to the Anadarko basin (Gehrels et al., 2011; Thomas, 2011; Chapman and Laskowski, 2019). It is possible, however, that small volumes of fine-grained arkosic sediment and metamorphic rock fragments could have been transported from the Sierra Grande/Apishapa uplifts of the Ancestral Rocky Mountains (Hills, 1963; Rascoe and Adler, 1983; Johnson, 1989; Hentz, 1992). These sediments are more common in the western portion of the craton (Gehrels, 2011; Chapman and Laskowski, 2019). Detrital grains from the Ancestral Rocky Mountains are derived from Yavapai-Mazatzal (1781-1657 Ma) Precambrian basement with smaller portions of 1500-1300 Ma grains derived from smaller granitoids (Gehrels, 2011). To the southeast of the Sierra Grande uplift lies the Bravo dome, which similarly exposed Precambrian basement rocks during the Pennsylvanian (Hills, 1963).

4.4 Eastern Sources

The eastern portion of the North American Craton is a structurally complex region comprised of multiple provinces of various ages. These include the Grenville (1300-950 Ma) province, accreted Gondwanan terranes (800-520 Ma), Iapetan synrift rocks (765-530 Ma), and synorogenic rocks of the Taconic (490-420 Ma), Acadian (420-350 Ma), and Alleghanian (330-

300 Ma) orogenies (Thomas, 2017). The influence of these grains is seen in the form of detrital zircon ages matching these timeframes as far west as Arizona and California (Gehrels, 2011; Chapman and Laskowski, 2019).

Rocks of the Grenville province include partially reworked crystalline rocks of the Granite-Rhyolite province, the Labrador province, and the Mars Hill terrane, as well as external and internal basement massifs (Thomas, 2017). Accreted Gondwanan terranes are comprised of Neoproterozoic metavolcanic, metasedimentary, and plutonic basement rocks that correspond to Pan-African-Brasiliano events (Thomas, 2017; Thomas, 2021). Iapetan synrift volcanic and plutonic rocks are exposed along Appalachian external basement massifs and are not distinguishable on the basis of age of zircons from Gondwanan accreted terranes (Thomas, 2017). Rocks of the Taconic, Acadian, and Alleghanian orogenic episodes represent arc-accretion events, eroded volcanic systems, granitic plutons, and recycling of late Paleozoic sandstones high in Grenville-aged sediments (Thomas, 2017).

4.5 Southern Sources

Potential sources also exist to the south of the study area in Gondwanan terranes accreted along the Ouachita-Marathon thrust belt. These include the Yucatan, Maya, Sabine, and Coahuila terranes (Martens, 2009; Thomas, 2019). The Marathon, Fort Worth, Arkoma, and Anadarko basins are known to contain grains originating from these sources; their detrital zircon age signatures typically contain significant amounts of Neoproterozoic and Appalachian-age grains (Thomas, 2016; Thomas, 2021). Grains from these sources will be further discussed in section **7.2**. A map of major North American basement age domains is shown in Figure 4.

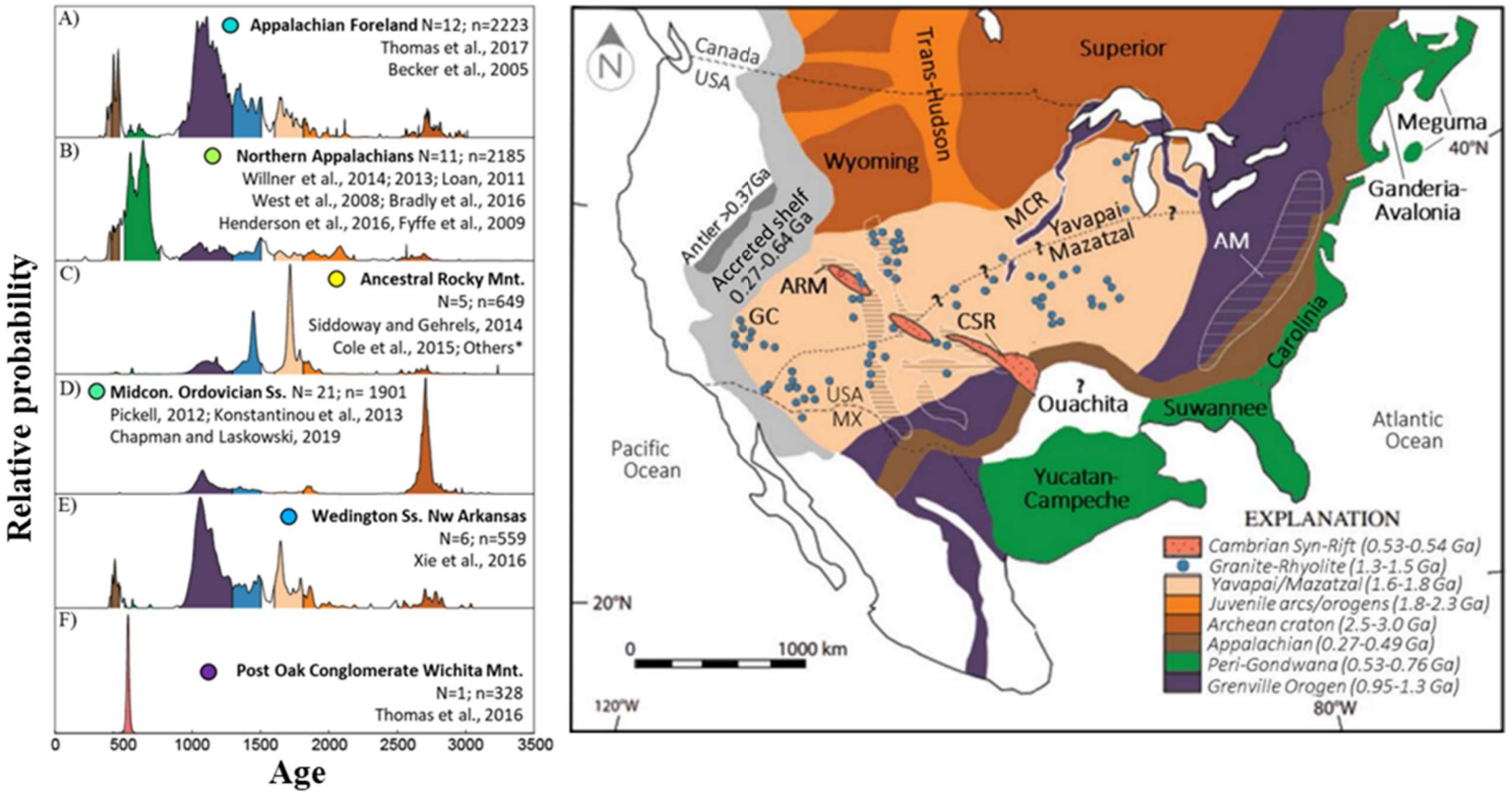

Figure 4. Basement map of major North American age domains (right) with representative detrital zircon age distributions for multiple domains color coded to map (left). Modified from Chapman and Laskowski (2019) and Tunin (2020).

CHAPTER V

METHODOLOGY

5.1 Detrital Zircon Geochronology

Analysis of isotope ratios of detrital zircons has emerged as a standard tool for sediment provenance studies. Since its early techniques in the 1960s, the methods and technology available to these analyses now allow for efficient and cost-effective age determinations from multiple single grain analyses at a precision and accuracy of 1-2% (Gehrels, 2014b). Detrital zircon geochronology allows for practical application of geochronologic ages to issues such as sediment provenance, sediment budgets, correlations between sedimentary units, and determinations of depositional age (Gehrels, 2014b; Saylor and Sundell, 2016; Saylor and Sundell, 2017). Recently, focus has been placed on the quantitative methods of interpreting data acquired from detrital zircon methods (Saylor and Sundell, 2016; Saylor and Sundell, 2017; Thomas, 2020). When coupled with detailed petrographic work, detrital zircon geochronology can shed light on potential sediment dispersal pathways that have significant implications on depositional models and siliciclastic reservoir distribution and quality.

The theory behind U-Pb detrital zircon studies has been well documented (most recently by Gehrels, 2014b) and will briefly be described here. Zircon is a powerful detrital grain for U-Th-Pb geochronology due to: (1) high U concentration; (2) moderate Th concentration; (3) U and Th being tightly held due to their similar size and charge; (4) low common Pb during

crystallization; (5) grows at 600-1100°C but retains Pb to >800°C, a significant property as this will generally record crystallization age; (6) common in felsic and intermediate igneous rocks; (7) chemically and mechanically resistant, and; (8) contains other elements that yield complementary information (e.g., Hf, Li, O, REE, He) (Gehrels, 2010b). The U-Th-Pb decay series consists of $^{238}U \rightarrow ^{206}Pb$ (half-life of 4.47 Ga), $^{235}U \rightarrow ^{207}Pb$ (half-life of 0.70 Ga), and $^{232}Th \rightarrow ^{208}Pb$ (half-life of 14.01 Ga). Respectively, these decay systems yield chronometers based on the measurements of $^{206}Pb/^{238}U$, $^{207}Pb/^{235}U$, and $^{208}Pb/^{232}U$ (Gehrels, 2014b). In practice, measured isotopes for zircon include $^{206}Pb/^{238}U$, $^{206}Pb/^{207}Pb$, and $^{206}Pb/^{204}Pb$; this is due to the lower Th concentration in zircons and the possibility that the Pb/Th system is decoupled from the Pb/U system, among other quantitative reasons. Of these essential ratios, $^{206}Pb/^{207}Pb$ and $^{206}Pb/^{204}Pb$ can be measured relatively easily with a mass spectrometer due to there being little or no fractionation of Pb isotopes during analysis (Gehrels, 2014b). However, measurement of $^{206}Pb/^{238}U$ proves more difficult, as Pb and U behave differently during analysis and are accordingly more fractionated. The method used in this study to correct for this was to measure the $^{206}Pb/^{238}U$ of three zircon standards of known ages (SL, FC-1, and R33 grains), compare the measured $^{206}Pb/^{238}U$ with the known $^{206}Pb/^{238}U$ to determine a correction factor, then using this correction factor to convert measured $^{206}Pb/^{238}U$ of unknown zircon grains to true $^{206}Pb/^{238}U$. Methodology concerning sample collection, preparation, and analysis will be covered in the following sections. Additional information on detrital zircon geochronology theory and methodology can be found in Gehrels (2010b, 2014b) as well as on the Arizona LaserChron Center website (https://sites.google.com/laserchron.org/arizonalaserchroncenter/home), where samples from this study were prepared and analyzed.

5.1.1 Sample Collection and Preparation

Samples for detrital zircon analyses were taken from core chips covering approximately 30 feet (9 meters) of Cleveland Sandstone section from the Magnolia Petroleum H. J. Schoenhals #1 well located in section 24, T. 21N, R. 26W, Ellis County, Oklahoma. Mapping of depositional sequences done by Hentz (2011) show that, like all other samples collected in this study for thin sections, core description, and more, these core chips indicate deposition within the Cleveland incised-valley fill as described in sections **2.1** and **3.2**. Eleven core chips were broken into approximately 1 in^3 pieces using a rock hammer, then crushed and disaggregated into sand-sized grains using a SPEX ShatterBox 8530 at Oklahoma State University. This produced about 3 kilograms of material that was sent to the University of Arizona LaserChron Center for separation and mounting. Separation involved the use of a Wilfley table to separate less dense minerals from high-density zircon using gravity separation (Pullen, 2011). Separation of higher density minerals was achieved through a hand magnet, Frantz magnetic separator, heavy liquids (diiodomethane), a Wig-L-Bug shaker, and acid washing (Simpson, 2012). The final zircon yield along with zircon standards SL, FC, and R33 were then mounted in a 1-inch diameter epoxy plug which was sanded down to a thickness of ~20 μm, polished, and imaged (Gehrels, 2010a).

5.1.2 U-Pb Age Analysis

Measurement of U-Th-Pb isotope ratios was conducted via laser ablation-inductively coupled plasma mass spectrometry (LA-ICPMS) at the University of Arizona LaserChron Center (ALC). Three-hundred fifteen (315) spots, each with a 20 μm diameter, were picked on individual zircon grains with the Chromium Offline Targeting software provided by the ALC. To aid in acquiring reliable ages, methods outlined in Gehrels (2014b) were applied to choosing these sites for laser ablation, including the use of cathodoluminescence (CL) and backscattered electron (BSE) images (Figure 5) to avoid fractures and complex crystal zonation and a semi-random

selection of grains. Samples were run with the ALC's Nu Plasma HR ICPMS coupled to a New Wave 193 nm ArF laser ablation system equipped with a New Wave SuperCell.

The two equations that solve for U-Pb ages are:

$$(1)\ T_{206/238} = \mathrm{Ln}\ (^{206}Pb^*/^{238}U + 1) / {}^{238}\lambda$$

$$(2)\ ^{206}Pb^*/^{207}Pb^* = 137.88[(e^{\lambda_1 t} - 1)/(e^{\lambda_2 t} - 1)]$$

The former calculates age based on the $^{206}Pb/^{238}U$ ratio, while the latter is based on the $^{206}Pb/^{207}Pb$ ratio. Methodology in place at the Arizona LaserChron Center uses the $^{206}Pb/^{238}U$ ratio to calculate the "best age" used in interpretation for zircons younger than 900 Ma and the $^{206}Pb/^{207}Pb$ ratio for ages older than 900 Ma. In both cases, it is necessary to correct for Pb loss that may occur due to high temperatures and/or subjection to hydrothermal fluids; the most common model for this correction is from Stacey and Kramers (1975), which is the method in use at the ALC. After correcting for Pb loss, correction for background ^{204}Hg is necessary, as this interferes with measurement of ^{204}Pb. This is accomplished through subtraction of ^{204}Hg based on the measurement of ^{202}Hg in proportion with the natural $^{202}Hg/^{204}Hg$ ratio of 4.32 (Gehrels, 2010a). Pit depth also affects the degree of fractionation measured, which is corrected for by regressing the measured ratios back to an initial value. Other more minor uncertainties arise from the decay constants of ^{238}U, ^{235}U, and ^{232}Th (known to be better than 0.3%, Steiger and Jäger, 1977), age of the FC-1 primary standard used to calibrate unknown zircons (in most cases better than 1%), and uncertainty in the composition of common Pb (Gehrels, 2010a).

Raw data from LA-ICPMS U-Pb analysis was converted to zircon ages using the Arizona LaserChron Centers "AgeCalc" software. For interpretation, only calculated zircon ages with >90% concordance were considered and zircons that may have inaccurate ages due to Pb loss or inheritance were disregarded. Filtering for 90% concordance reduced data from 315 calculated ages down to 270 ages. These data were then presented graphically using the Arizona LaserChron

Center's "Normalized Age Probability Plots" software, and age peaks were identified with the ALC's "Age Pick" software.

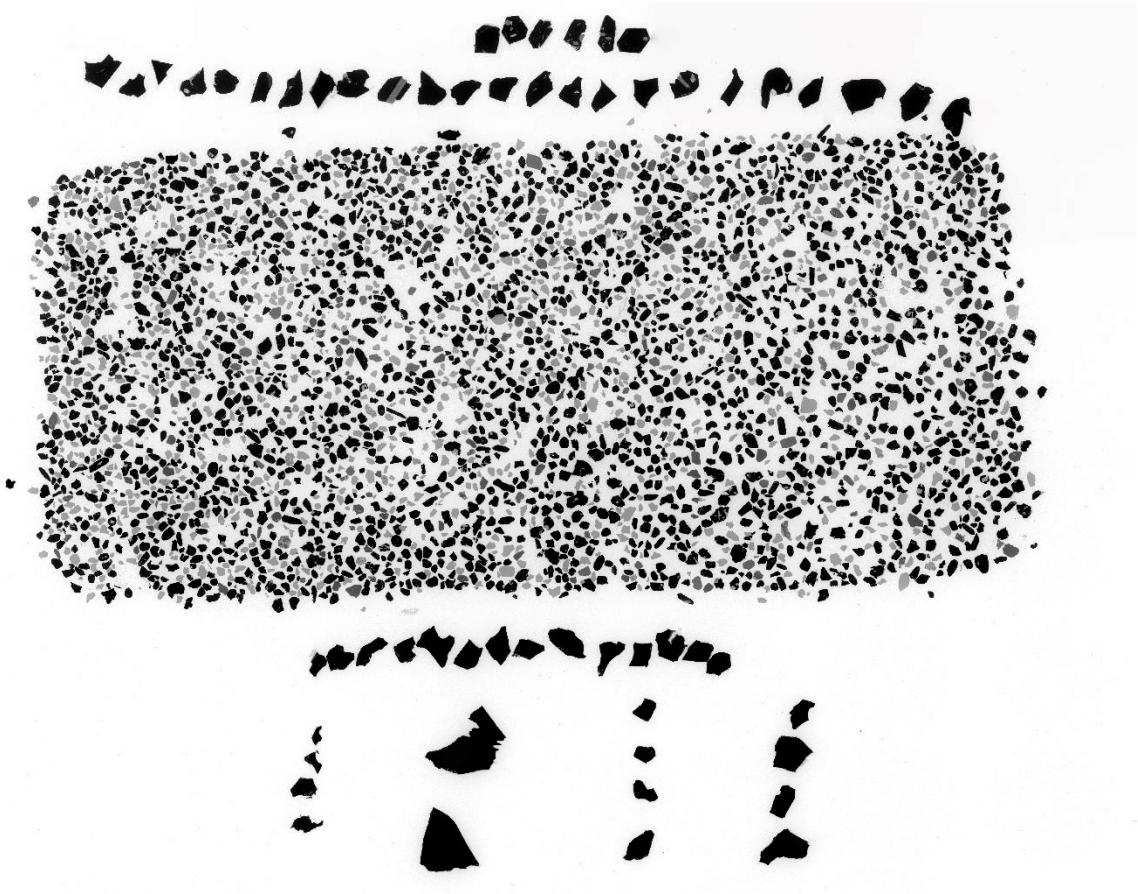

Figure 5. Inverted backscattered electron image of the zircon mount analyzed in this study. Large grains at top and bottom of image are zircon standards in use at the Arizona LaserChron Center; grains in the middle of the image are from the Cleveland interval analyzed.

5.1.3 Hafnium Isotopic Analysis

The hafnium (Hf) isotope system is based on the decay of ^{176}Lu to ^{176}Hf ("Hf analytical methods at the Arizona LaserChron Center (University of Arizona)"). During the crystallization of zircon in magma melts, zircons take up relatively large amounts of Hf but exclude lutetium (Lu), making the $^{176}Hf/^{177}Hf$ isotope ratio a useful chronometer in geochronologic studies. Hafnium isotope analyses are useful when two sediment sources have overlapping zircon

crystallization ages as determined from U-Pb analysis, as the Hf signatures reveal compositional differences in magma (Thomas et al., 2016). In this study, Hf isotopic analyses were conducted to attempt to distinguish between detrital zircons with ages of 535 ± 10 Ma, which may correspond to either Cambrian synrift igneous rocks (539-530 Ma) or Gondwanan accreted terranes exposed in the Appalachian Mountains (700-530 Ma).

Hafnium isotopic analysis was conducted at the Arizona LaserChron Center utilizing the same instrumentation described in **5.1.2**. Thirty spots were chosen for analysis via laser ablation. These were directly on top of existing pits created during U-Pb age analysis; these spots were chosen to evenly represent the main age groups and avoid grains with discordant ages. Instrument parameters were set based on a Hf standard solution (JMC475) as well as zircon standards Mud Tank, Temora-2, FC-52, 91500, Plesovice, R33, and SL2. The $^{176}Hf/^{177}Hf$ at the time of crystallization is calculated from the measurement of present-day $^{176}Hf/^{177}Hf$ and $^{176}Lu/^{177}Hf$ using the decay constant of ^{176}Lu ($\lambda = 1.867e^{-11}$, from Scherer et al., 2001; Söderlund et al., 2004) via the following equation ("Hf analytical methods at the Arizona LaserChron Center (University of Arizona)"):

$$(^{176}Hf/^{177}Hf)^t = (^{176}Hf/^{177}Hf)^0 - (^{176}Lu/^{177}Hf)^0 * (e^{\lambda t} - 1)$$

Hafnium data are reported in epsilon units (ε) as the mean and 1σ standard error. Results are reported as εHf(t), where t is the time of crystallization based on U-Pb analysis.

5.2 Sandstone Petrology

Petrographic analysis of sixteen thin sections from four different wells was conducted to qualitatively and quantitatively assess detrital mineral composition and abundance. Emphasis was also placed on describing porosity development and paragenesis. More than 300 points were

counted per thin section, and constituent values were normalized for plotting on a Folk (1968) QRF diagram and Dickinson (1983) provenance type ternary diagram. Photomicrographs for an additional five wells were acquired from the Oklahoma Petroleum Information Center (OPIC), and thin sections from well cuttings were created for an additional nine wells; while these sections could not be point counted, they still provided useful insight into Cleveland Sandstone petrology.

One core from the Petroleum Inc. Neidens 1-10 well located in section 10, T. 20N, R. 26W was described at the Oklahoma Petroleum Information Center (OPIC) in Norman, Oklahoma. Over 100 feet (30 meters) of Cleveland Sandstone section was described. Additional data, including a full log suite, thin section photomicrographs, and routine core analysis (RCA) and x-ray diffraction (XRD) data from core plugs, allowed for further insights into the formation's composition and fabric. Locations of the various data sources are shown in Figure 6.

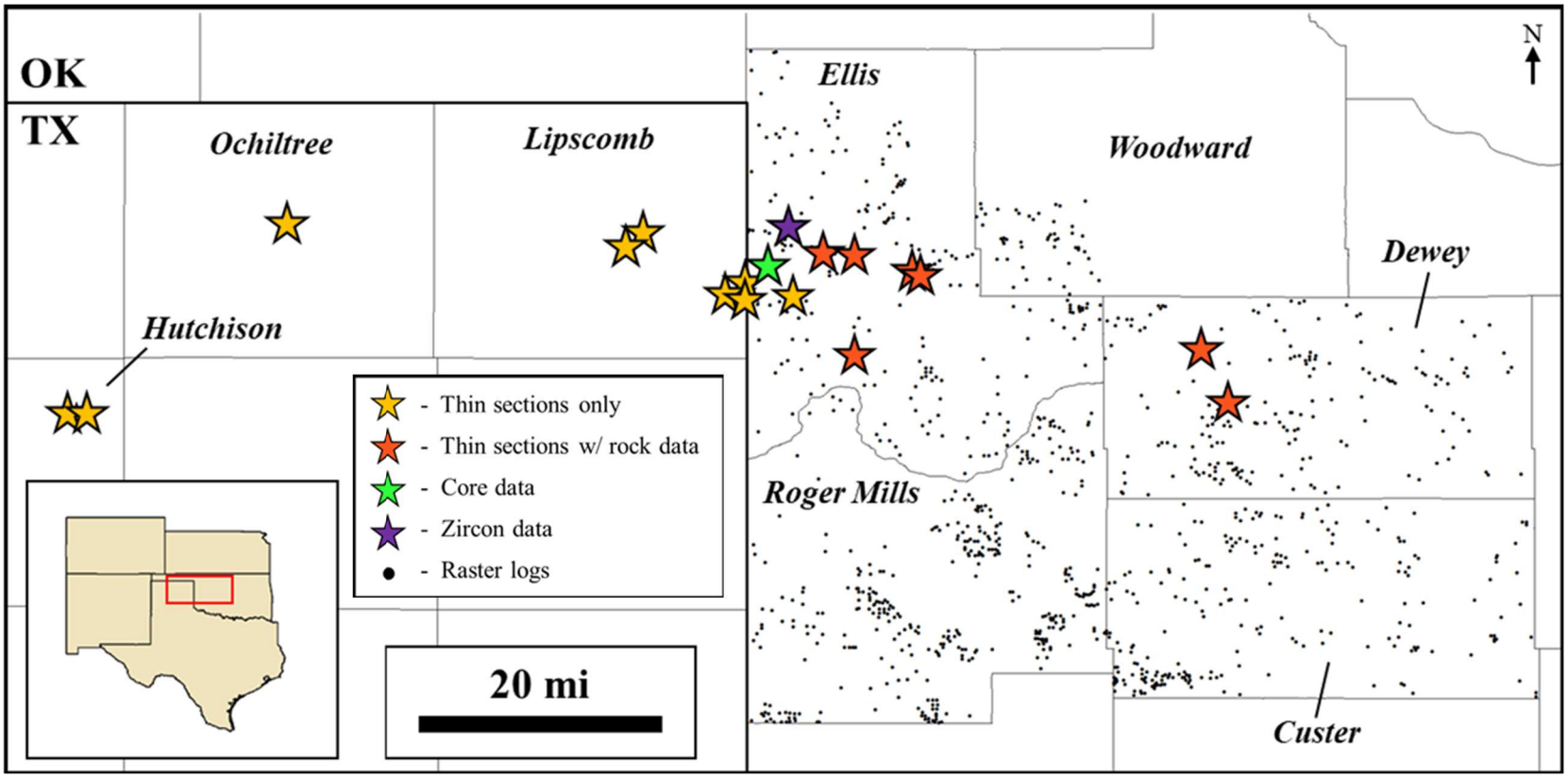

Figure 6. Location and description of data acquired for the study. Labels are county names.

CHAPTER VI

RESULTS

6.1 Cleveland Sandstone Petrology

Description of Cleveland Sandstone petrology in the study area was accomplished through thin section analysis and core description. Where relevant, results from other studies will be noted to allow for comparison in the following chapter. Point counting allowed for sandstone classification according to the Folk (1968) classification and construction of a paragenetic sequence of diagenetic events; results are shown in Figures 7, 8 and 9.

Of the sixteen thin sections classified via point counting, ten samples were classified as litharenites, five were classified as feldspathic litharenites, and one sample was classified as a sublitharenite. Quartz was the most common detrital constituent, ranging from 35-75% of the rock fabric with an average of 66%. Quartz grains were predominantly monocrystalline, subangular-subrounded, poorly- to well-sorted and had sizes between 0.08-0.125 mm (very-fine to fine-grained), with a few samples having a significant amount of silt-sized grains (0.05 mm). Sorting and texture of sand grains, as well as samples having little (< 5%) to no clay, indicate a submature to mature sandstone.

Rock fragments were a larger portion of rock composition for all samples compared to samples from Bacon (2012) located in Oklahoma County, Oklahoma; quartz was more abundant in Bacon (2012) samples. Abundance of rock fragments ranged from 19-62%, with an average of28%. Roughly 80% of the rock fragments observed in samples from this study were metamorphic rock fragments, while rock fragments of the formation in north-central Oklahoma are primarily chert (Bacon, 2012). Other rock fragments identified in samples from this study were shale rock fragments, chert, and mica fragments. Samples from Hentz (1992) also show an abundance of metamorphic rock fragments, though tend to be more feldspathic (Figures 8 and 9). Feldspar in samples from this study occur in the form of plagioclase; no microcline was observed in any samples. Other minerals observed in minor amounts were tourmaline, pyrite, and scattered organic matter.

Porosity occlusion in samples from this study was primarily in the form of quartz overgrowths, with minor amounts of pseudomatrix, created due to deformation of metamorphic rock fragments, also occluding porosity. Calcite cementation is the dominant porosity occluding process in Bacon (2012) samples and was not observed in any samples from this study; however, this is almost certainly due to selective sampling, where ideal reservoir intervals lacking calcite cement were selected for data collection. XRD data, RCA data, and well log data indicate that calcite does occur in significant amounts in some non-reservoir intervals for multiple wells in the study area, supporting the selective sampling conclusion as to why no calcite cement was observed in thin sections from this study. In both this study as well as Bacon (2012), secondary porosity created from the dissolution of rock fragments and feldspars is the most common form of porosity; primary porosity in most samples is virtually eliminated due to quartz overgrowths and/or pseudomatrix. Porosity values determined through point counting ranged from 1-15% with an average of 7.7%.

A paragenetic sequence was created to describe and summarize observations noted across all samples. The sequence, shown in Figure 7, is summarized as follows: (1) early clay lining of quartz grains, in some cases deterring syntaxial overgrowth generation; (2) quartz overgrowths occurring before compaction creating pseudomatrix from metamorphic rock fragments, evident because pseudomatrix forms around existing overgrowths; (3) dissolution of rock fragments and feldspars creates intragranular and moldic secondary porosity and continues throughout the diagenetic process; (4) chloritization of clays; (5) later formation of authigenic clays lining secondary pores; (6) late dissolution of quartz, evident in corroded quartz grains. As with the creation of many paragenetic sequences, it is difficult to exactly determine the onset of these diagenetic events, and much overlap occurs.

In addition to the sixteen thin sections acquired from core that were point counted, thin sections from cuttings were acquired for an additional nine wells, and photomicrographs were acquired for an additional four wells. These allowed for insights into Cleveland Sandstone composition in Dewey County, Oklahoma and the Texas Panhandle, as all thin sections that were point counted were located in Ellis County, Oklahoma. Samples in Dewey County, Oklahoma displayed low amounts of feldspar, similar to samples located in Ellis County. However, lithic fragments were less common, with quartz being a larger percentage of rock composition. Schistose metamorphic rock fragments were still the dominant lithic fragment, and micas were observed throughout the photomicrographs in samples from Dewey County. Quartz grains in samples from Dewey County were again subangular-subrounded, but were slightly more well-sorted than samples from Ellis County. Quartz grains in samples from Dewey County were also noted to show a slight reduction in grain size, though would still be classified as very-fine grained (0.08-0.125 mm). Calcite cement was common in samples from Dewey County and is occasionally replaced by dolomite. Porosity values in these samples, taken from core plugs, ranged from 2.0% to 7.3% and was dominantly in the form of secondary porosity. Despite only

having photomicrographs, all aspects of the paragenetic sequence created in this study were identified in samples from Dewey County.

Thin sections made from cuttings were studied for six wells in the Texas Panhandle. These samples contained angular-subangular quartz grains with an average size of 0.25 mm (fine- to medium-grained), a significant increase from samples in Oklahoma. Various rock fragments were identified; these included siltstone fragments, shale fragments, volcanic rock fragments, and carbonate rock fragments. The presence of volcanic and carbonate rock fragments is odd, as these were not observed to any degree in samples in Oklahoma, nor are they spoken of in any published literature. These lithic fragments may not represent actual Cleveland Sandstone composition, but may have initially been part of an adjacent stratigraphic unit that had not yet been cycled out of the drilling fluid at the time cutting samples were acquired. Composition plotted on the Dickinson (1983) provenance diagram (Figure 10) showed a recycled orogenic origin for most detrital grains.

The Neidens 1-10 core provided useful insight into sedimentary processes shaping the Cleveland Sandstone reservoir. Six main core-scale lithotypes were identified: (1) rounded clay pebble conglomeratic sandstone; (2) ripple laminated sandstone; (3) cross-laminated sandstone; (4) massively bedded sandstone; (5) interbedded sandstone and shale; (6) horizontally laminated sandstone. Representative core photographs can be found in the Appendix, along with XRD and RCA data for multiple core plugs. Other less abundant sedimentary structures included horizontal burrows in shalier portions, planar “pinstripe” lamination, wavy lamination, and flaser bedding. Sandstone observed in the Neidens 1-10 core was light gray and very-fine grained. Interestingly, all lithotypes identified in the Neidens 1-10 core were also present in core descriptions of the formation in Pawnee County, Oklahoma (Cain, 2017).

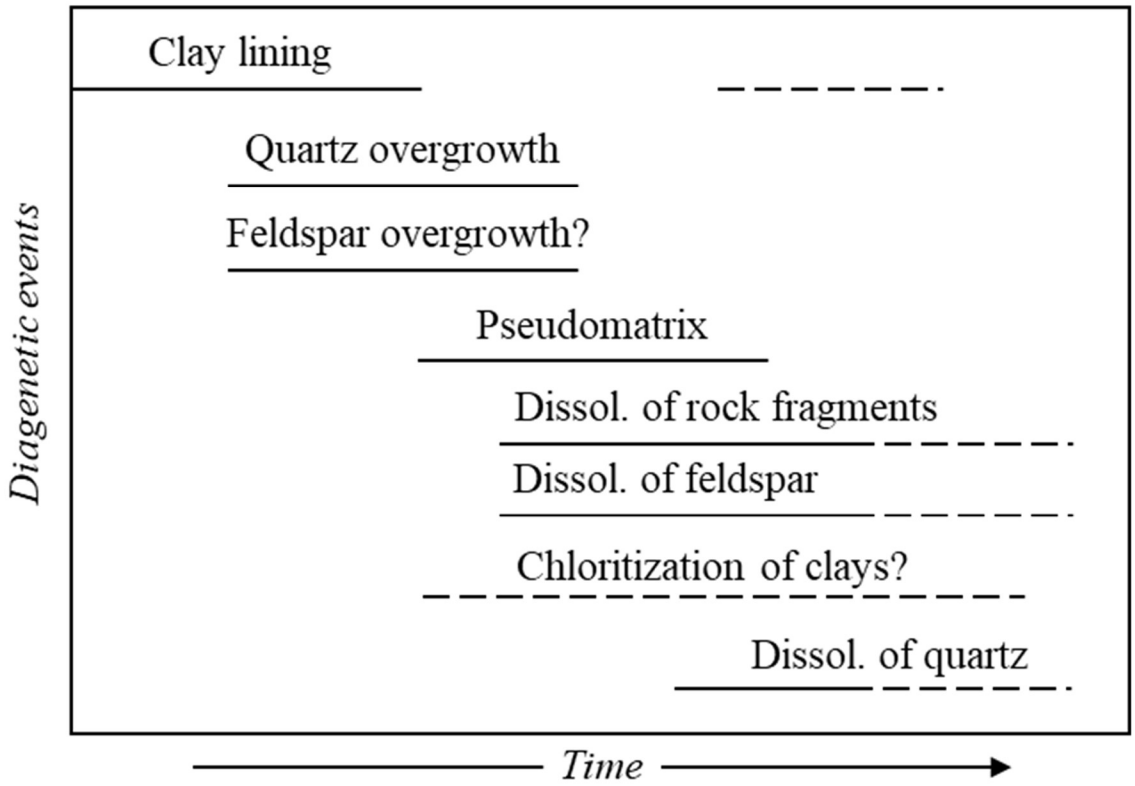

Figure 7. Paragenetic sequence created to describe timing of diagenetic events in the Cleveland Sandstone. Note that this sequence was created as a broad description of the formation's diagenetic history, and incorporates observations from all thin sections.

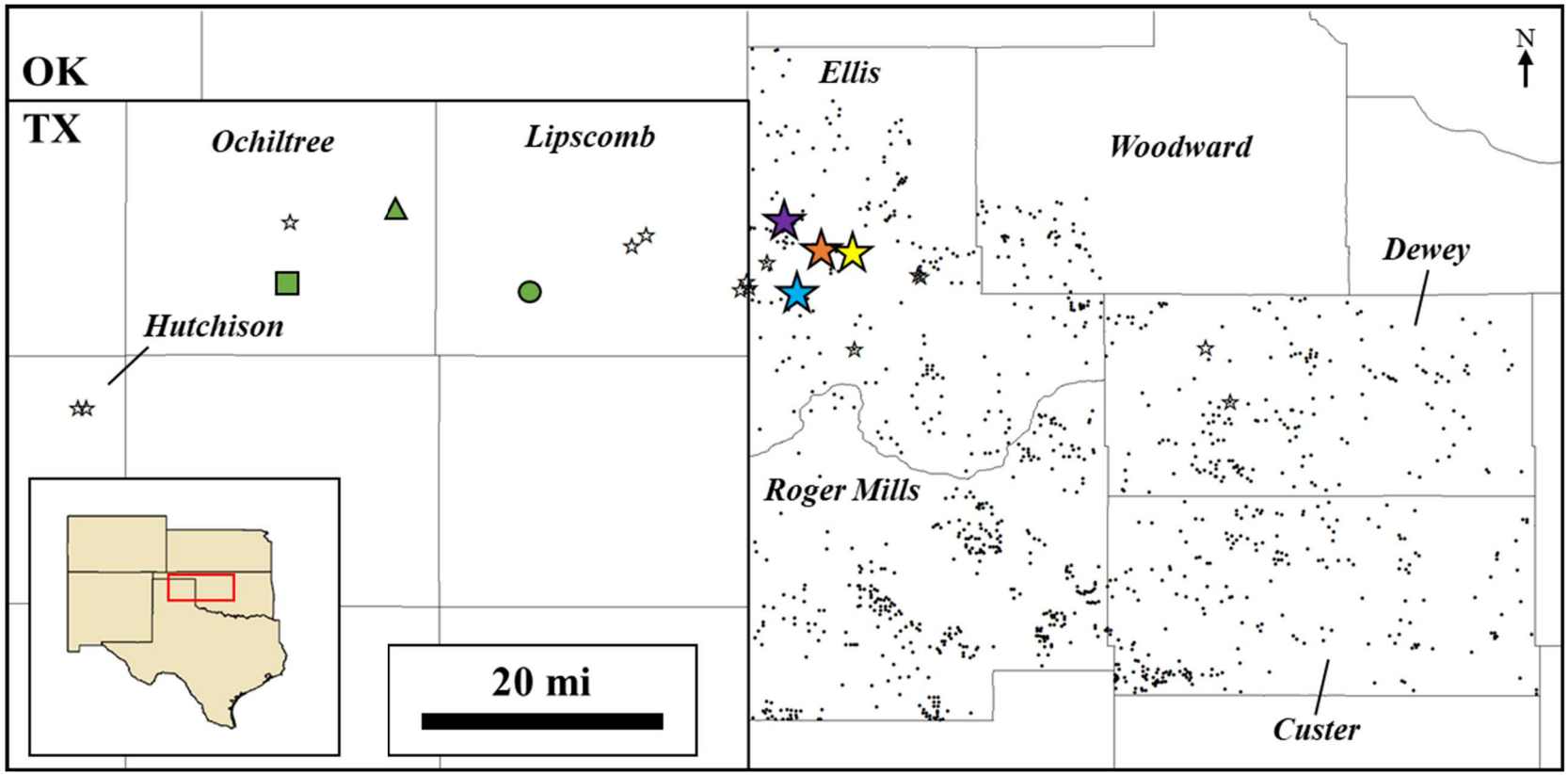

Figure 8. Location of thin sections point counted and classified according to Folk (1968) in this study (stars) and by Hentz (1992).

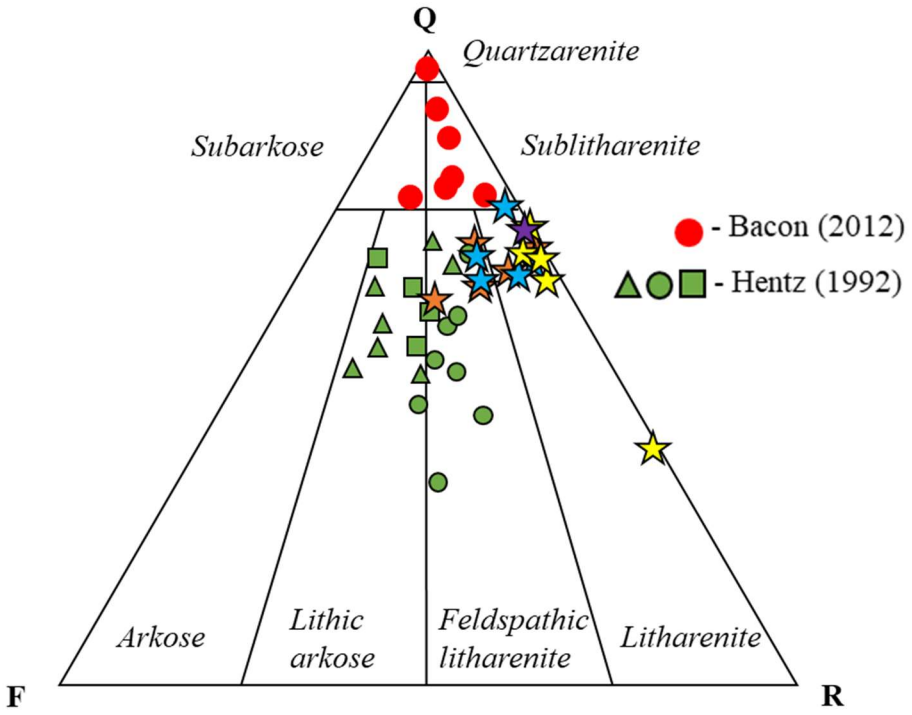

Figure 9. Results of point counting color-coded by location to Figure 7 and plotted on a Folk (1968) QRF diagram.

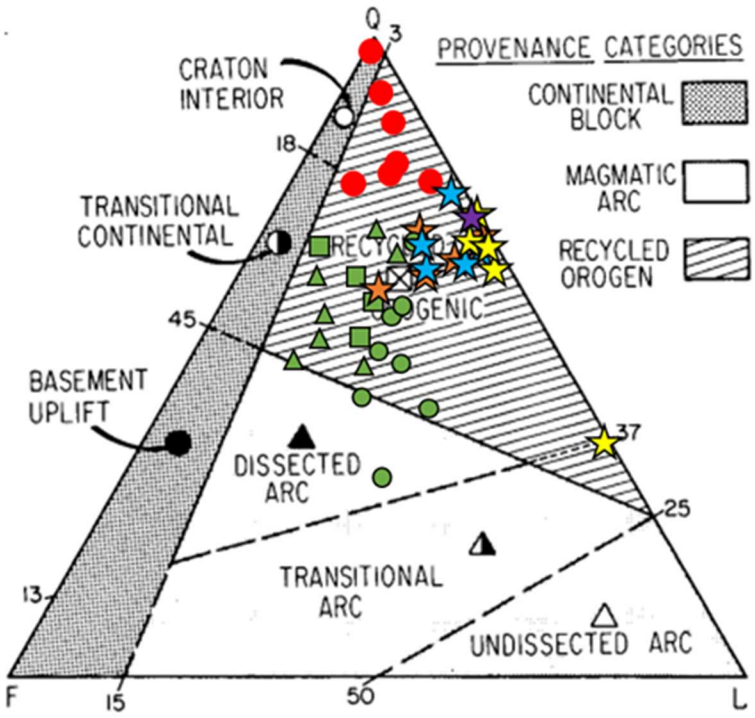

Figure 10. Results of point counting plotted on a Dickinson (1983) diagram.

6.2 Detrital Zircon Age Signature

6.2.1 U-Pb Data

After filtering data based on concordance, ages calculated from the U-Th-Pb series ratios ranged from 308 Ma to 2836 Ma. With Grenville ages included, Appalachian (490-270 Ma) grains accounted for 9% of ages, Neoproterozoic (750-530 Ma) grains for 18%, Grenville (1300-950 Ma) grains for 40%, Granite-Rhyolite (1500-1300 Ma) grains for 13%, Yavapai-Mazatzal (1800-1600 Ma) grains for 6%, and Archean Craton (>2500 Ma) grains for 2%. Due to the prevalence of Grenville-age grains in Paleozoic sandstones throughout North America, abundance of age groups was also considered excluding these grains. Excluding Grenville-age grains, Appalachian grains accounted for 15% of ages with a peak (11 grains) at 416 Ma, Neoproterozoic grains for 30% with peaks at 601 Ma and 619 Ma (16 and 14 grains, respectively), Granite-Rhyolite grains for 21% with minor peaks at 1377 Ma and 1452 Ma (11 and 12 grains, respectively), Yavapai-Mazatzal grains for 10%, and Archean Craton grains for 4%. Peaks within the Grenville ages are present at 1037 Ma, 1142 Ma, and 1166 Ma (32, 25, and 25 grains, respectively).

6.2.2 Hafnium Data

Distribution of εHf(t) values provides important information about magma composition that allows for differentiation between a Laurentian and Gondwanan source for some age groups. Data were plotted with HafniumPlotter, a MATLAB algorithm developed at the University of Arizona using kernel bandwidths of 150 Ma for the x-axis and 3ε for the y-axis. Of the 30 spots selected for analysis, 27 yielded usable results; these are plotted in Figures 11 and 12. Discussion of Hf results will take place in the following chapter.

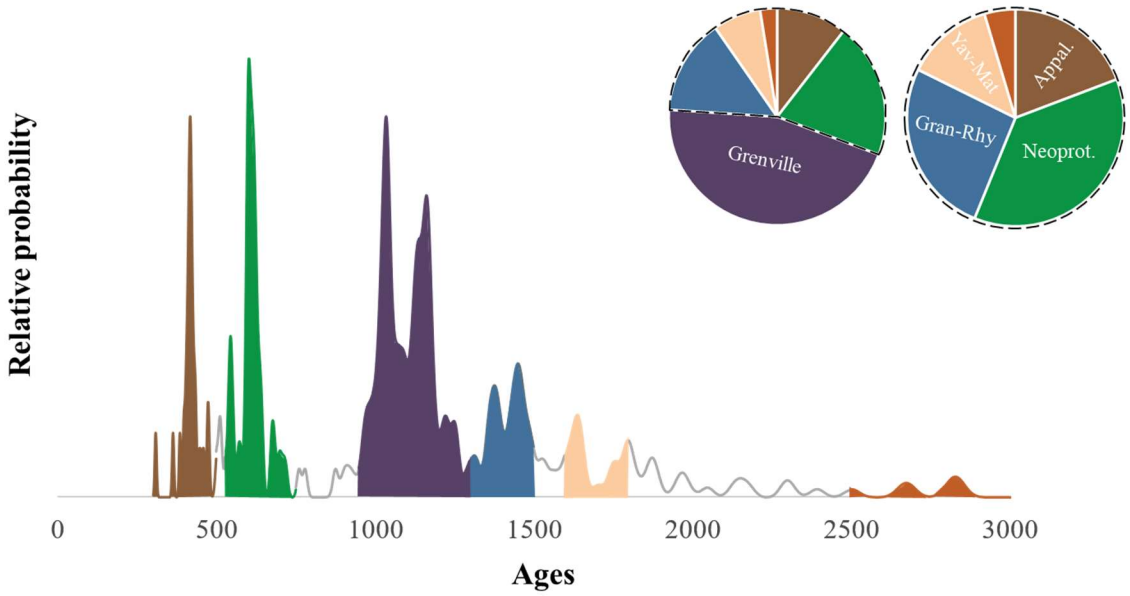

Figure 11. Normalized probability distribution of ages calculated from U-Pb detrital zircon data. Color-coded to Figure 3.

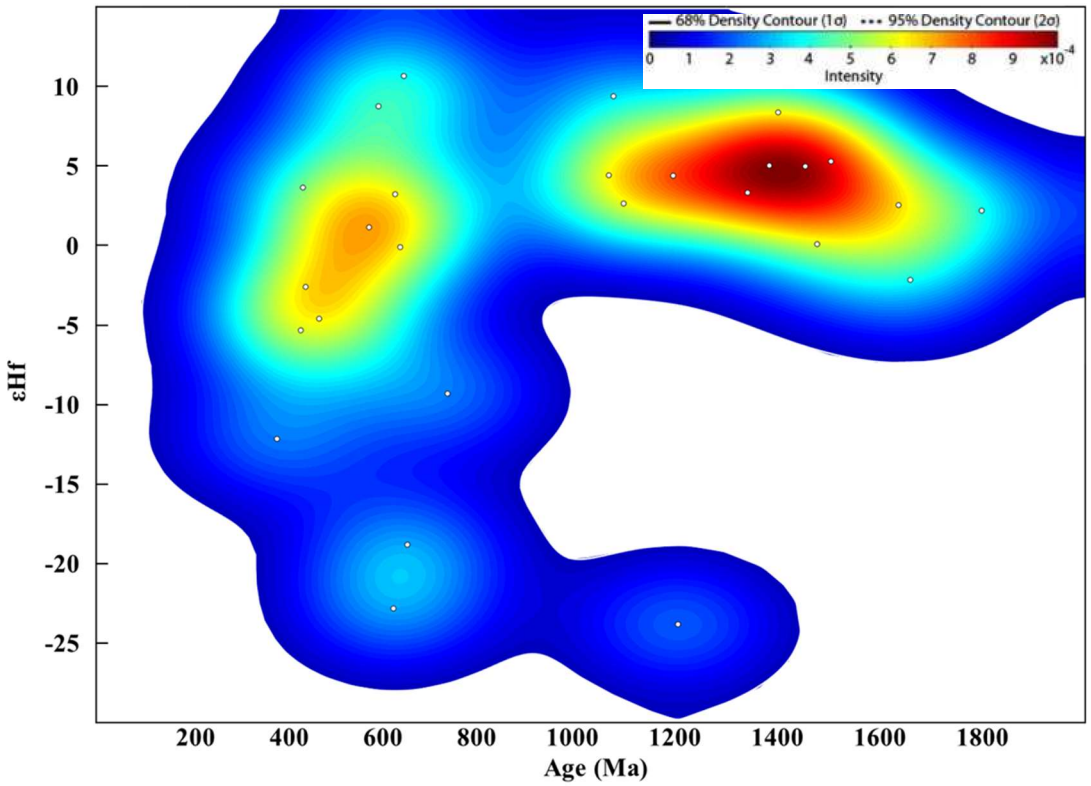

Figure 12. 2-D plot of bivariate kernel density estimates using parameters described in **6.2.2**.

CHAPTER VII

DISCUSSION

7.1 Comparative Petrology

7.1.1 Texas Panhandle

The Cleveland Sandstone as observed in the study area in western Oklahoma is fairly similar to that of the formation in the Texas Panhandle as studied by Hentz (1992, 1994, 2011, 2015) with a few key differences. These differences are interpreted to support Hentz (1992, 2011) in his conclusion that the fluvial system that created the incised fluvial valley of the Cleveland formation flowed from west to east in the Texas Panhandle region. Samples from Hentz (1992) and Hentz (2011) displayed more feldspars than were present in thin sections available to this study. This supports a west-east trending fluvial system, as these feldspars would be expected to weather out of the system downdip in western Oklahoma where samples from this project were acquired. Thin sections from Hentz (1992) had an average porosity of 2.8% compared to 7.7% in the samples from this study; however, the wells from which these samples were taken were non-productive in the Cleveland interval. If average porosity were to be lower in the Texas Panhandle versus western Oklahoma, one might interpret this as supporting the west-east trend, as increasing sandstone maturity to the east and weathering of grains (such as feldspar) creates superior reservoir conditions. Alternatively, feldspar content could have initially been similar in the two regions but dissolution of these grains in western Oklahoma was more prevalent.

Samples from this study in Dewey County further support a west-east trend in Cleveland Sandstone deposition. Compared to samples updip in Ellis County, samples show an increase in quartz content with slightly better sorting and a slight decrease in grain size, while still containing few feldspars. These observations indicate a slightly more mature sandstone, which in turn indicates a slightly longer transport distance for detrital grains.

7.1.2 Cherokee Platform

Comparison of the Cleveland Sandstone of the study area with the formation in north-central Oklahoma on the Cherokee Platform was accomplished by considering petrographic work by Bacon (2012) and Cain (2017), who primarily utilized thin sections and core and outcrop data, respectively (Figure 13). As discussed in section **2.1**, the Cleveland Sandstone has been better studied where it occurs on the Cherokee Platform; oddly, however, few petrographic studies of the formation exist. Exceptions include early studies by Baker (1958), Cary (1955), and Clare (1963).

Samples from Bacon (2012) have several key differences to the samples analyzed in this project. Bacon (2012) samples were primarily classified as sublitharenites, with one sample classified as a subarkose and two samples classified as quartzarenites. All samples, then, had a higher quartz content than the samples from this study. Perhaps most interesting about samples from Bacon (2012) is the lack of metamorphic rock fragments, which were “very miniscule” in samples from his study; while lithic fragments were a common detrital constituent in his samples, these fragments were predominantly chert. Chert was very rare in samples from this study, indicating a chert-rich source that contributed sediment to the Cleveland formation as it occurs on the Cherokee Platform, but not to the formation in the western Anadarko basin. Such a source could be Mississippian rocks subaerially exposed along the Nemaha Ridge during Cleveland time

(Turnini, 2019); mapping of the Cleveland Sandstone by Bacon (2012) indicates a from-the-north sandstone distribution in Kingfisher County, Oklahoma, located approximately 20 miles south of the Nemaha Ridge. Chert-bearing Mississippian rocks were also uplifted and exposed during Cleveland time in the Ouachita uplift (Campbell, 1997).

Glauconite, absent in samples from this study, was present in samples from Baker (1958) and Bacon (2012). The presence of glauconite is frequently interpreted as an indicator for a marine, shallow water environment (Triplehorn, 1965). Samples containing glauconite in these studies were likely deposited in a prodelta environment where marine influence allows for the formation of glauconite, whereas samples from this study indicate deposition within a lowstand incised fluvial valley based on the following observations: 1) juxtaposition of fluvial sandstone on interpreted transgressive systems tract deposition in the Neidens 1-10 core with estuarine/tidal deposits at top of core; 2) sample locations falling within incised valley as mapped by Hentz (2011), and; 3) hydrocarbon production trends and (when available for samples) well log data indicating channel-fill sandstones.

Outcrop, core, and thin section work by Cain (2017) further characterizes the Cleveland Sandstone on the Cherokee Platform. Eight lithotypes were identified at the outcrop- and core-scale and were also classified via qualitative thin section petrography. Of these eight lithotypes, the Neidens 1-10 core examined in this study contained six of these distinct lithotypes; these were: 1) interbedded sandstone and shale; 2) ripple laminated sandstone; 3) horizontally laminated sandstone; 4) planar cross-laminated sandstone; 5) massive sandstone, and; 6) rounded clay pebble conglomeratic sandstone. While Cain (2017) does not provide percentages of detrital constituents or sandstone classifications for sandstone-rich lithotypes, qualitative descriptions are given. Oddly, Cain (2017) mentions metamorphic rock fragments to be a major part of rock composition in the ripple laminated sandstone and massive sandstone lithotypes, while only mentioning chert once as a minor constituent of the planar cross-laminated sandstone lithotype.

Proximity to chert-rich sources could be responsible for the discrepancies in chert content between Bacon (2012) and Cain (2017), although the lack of geochronologic data for the Cleveland formation leads to many assumptions about provenance and sediment dispersal that requires further investigation before definitive conclusions on sediment pathways are made for the formation in north-central Oklahoma.

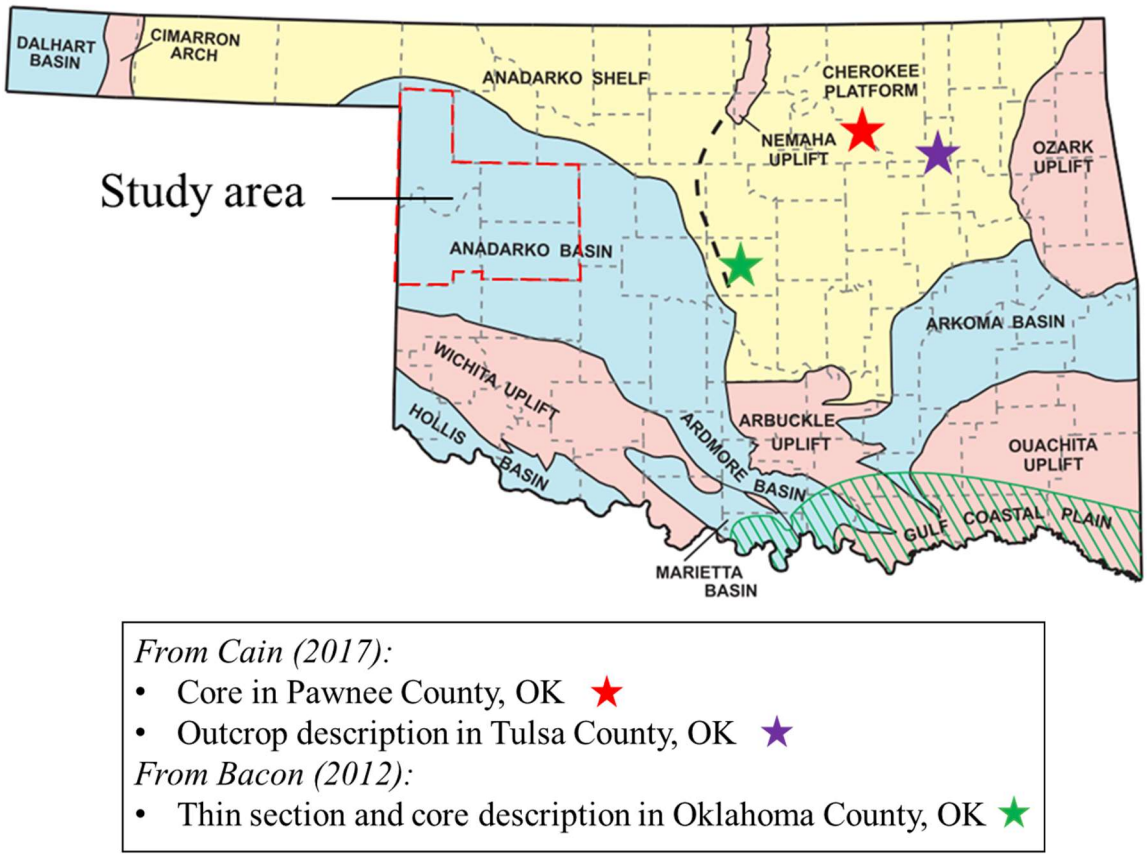

Figure 13. Location of Bacon (2012) and Cain (2017) samples. Modified from Johnson (2008).

7.2 Potential sources

New detrital zircon data acquired for this study necessitates a new sediment dispersal reconstruction for the Cleveland Sandstone in the western Anadarko basin. The initial hypothesis for this study was that sediment supply to the formation was primarily from the adjacent Amarillo-Wichita uplift and Ancestral Rocky Mountains, consistent with the interpretation of Hentz (1992), as well as a possible Appalachian influence. Ages for the one sample acquired in this study suggest only minor contributions from these sources, with a more complex sediment dispersal only recently documented in the literature. What follows is a discussion of U-Pb age results organized by age.

7.2.1 Archean and Paleoproterozoic (>1800 Ma)

Grains with a calculated age >1800 Ma were not common in the one sample analyzed, making up only 4% of the population. These grains span a few different tectonostratigraphic provinces, namely the Penokean (1900-1800 Ma), Trans-Hudson (2000-1800 Ma), and Superior (>2400 Ma) provinces. Superior-age detrital zircons are relatively abundant in Ordovician passive-margin off-shelf sandstones which were deposited along the rifted margin of Laurentia and were exposed in the Ouachita thrust belt during the Late Paleozoic, including the Wichita and Arbuckle uplifts (Thomas, 2016; Thomas, 2021). Such grains dominate U-Pb detrital zircon age distributions in the Late Pennsylvanian Vanoss Conglomerate in the Anadarko basin (Thomas, 2021). A Gondwanan source, the Moroni-Itacaiunas province, also contains grains ranging from 2224-1945 Ma (Thomas, 2021). Recycling of these quartzose Ordovician sandstones in the Anadarko basin could be responsible for the few grains observed in the >1800 Ma age range, and/or recycling of other sandstones containing grains of the Trans-Hudson, Penokean, and/or Moroni-Itacaiunas provinces contributed the small population observed in the Cleveland sample from this study.

7.2.2 Late Paleoproterozoic (1800-1600 Ma)

Late Paleoproterozoic grains correspond to the Yavapai-Mazatzal province and make up 6% of the sample analyzed in this study. These grains were exposed and eroded via uplift of the Ancestral Rocky Mountains, which had likely reached their maximum height during the Middle Pennsylvanian prior to Cleveland Sandstone deposition (Xie, 2018). Grains in this age range were also exposed in Precambrian basement rocks along the Nemaha ridge; however, these exposures were covered prior to deposition of the Cleveland Formation (Moore, 1979). The lack of Late Paleoproterozoic grains suggests that the Ancestral Rocky Mountains were not a major contributor of sediment to the Cleveland Sandstone in the western Anadarko basin.

7.2.3 Early Mesoproterozoic (1600-1300 Ma)

Grains ranging from 1600-1300 Ma correspond to the Granite-Rhyolite province in the midcontinent located to the southeast of the Yavapai-Mazatzal province and accounted for 13% of grains in the one sample analyzed. Anorogenic high-silica magmatism emplaced several plutons throughout the North American midcontinent that yield U-Pb zircon ages ranging from 1500-1300 Ma (Whitmeyer, 2007; Xie, 2018). Basement rocks exposed by the Arbuckle uplift also belong to the Granite-Rhyolite province (Thomas, 2016). The Rondonia-San Ignacio component of Gondawana contains grains ranging in age from 1564-1339 Ma and contributes sediment to sandstones throughout the Marathon foreland (Thomas, 2019). Finally, passive-margin off-shelf sandstones deposited around the Ouachita embayment and subsequently exposed and eroded along the Ouachita thrust belt contain abundant Granite-Rhyolite-age grains, providing a potential source of recycled grains (McGuire, 2017; Thomas, 2021).

Excluding Grenville-age grains, Early Mesoproterozoic grains were the second most abundant age group behind Neoproterozoic grains. Peaks in 1600-1300 Ma grains in the sample

from this study occur at 1377 Ma and 1452 Ma, with 11 and 12 grains, respectively. A sample from the Rush Springs Sandstone in the Anadarko basin also displays a mode at 1377 Ma, and a sample from the Garber Sandstone in the Anadarko basin displays a mode at 1384 Ma (Thomas, 2021). Atokan sandstones with a northeastward dispersal in the Arkoma basin (as determined by paleocurrent analysis, further discussed in **7.2.5**) have a secondary mode at 1455 Ma, and samples from the Wellington Formation in the Anadarko basin also display a minor peak at 1453 Ma (Sharrah, 2006; Thomas, 2021). Due to the overlap of ages with Laurentian- and Gondwanan-derived Early Mesoproterozoic grains, it is difficult to attribute these grains to a specific source.

7.2.4 Middle to Late Mesoproterozoic (1300-950 Ma)

Middle to Late Mesoproterozoic grains were the most abundant age group in the one sample analyzed in this study, making up 40% of the population. Such grains are abundant in many sandstones throughout North America and in many cases are likely not first-cycle zircons (Becker, 2005; Sharrah, 2006; McGuire, 2017; Xie, 2018). This age group has a few potential sources, including the Grenville province in eastern Laurentia as well as in peri-Gondwanan terranes such as the Maya and Coahuila blocks (Martens, 2009; Xie, 2018; Thomas, 2019). Distinguishing between these sources is not possible on the basis of U-Pb zircon ages alone due to overlap of values; this, along with the widespread abundance of Grenville-age zircons throughout North America, generally render grains of these ages ineffective at determining the provenance of the sample in this study. However, recent εHf data suggests that Grenville-derived zircons typically display dominantly positive values, while Amazonian-derived zircons may include more negative values (Thomas, 2019). εHf values for 1300-950 Ma zircons in this study ranged from +2.5 to +9.2 with the exception of one grain at 1174 Ma with a value of -23.9; while

not conclusive, the overall lack of negative εHf values in this age range may suggest that these grains were derived from the Grenville province for the sample analyzed in this study.

7.2.5 Neoproterozoic to early Paleozoic (790-530 Ma)

Grains ranging in age from 790-530 Ma have potential sources in Pan-African/Brasiliano basement rocks in Gondwanan accreted terranes (800-530 Ma) and Iapetan synrift igneous rocks (765-530 Ma), including those exposed by the Wichita uplift (539-530 Ma) (Thomas, 2012; Thomas, 2020). These grains accounted for 18% of ages for the one sample analyzed in this study; excluding Grenville-age grains, they accounted for 30%, with peaks at 601 Ma and 619 Ma. The sample analyzed in this study only contained three grains with ages corresponding to eroded Wichita uplift rocks; this has major implications on Cleveland sediment dispersal, as unlike other formations proximal to the uplift (i.e. Post Oak Conglomerate, Thomas, 2016), the lack of these grains suggests little to no contribution from the nearby Wichita uplift.

Excluding Grenville-age grains, Neoproterozoic grains were the most abundant age group in the Cleveland sample analyzed in this study. Samples from several studies discussing Appalachian-derived detritus typically have small populations of Neoproterozoic grains (Thomas, 2004; Becker, 2005; Thomas, 2017; Chapman and Laskowski, 2019; Thomas, 2020; Thomas, 2021). Exceptions include some samples in the northern Illinois basin and the Forest City basin, where peri-Gondwanan terranes accreted proximal to the Northern Appalachian region are interpreted to have intermittently contributed these grains (Thomas, 2020). Neoproterozoic grains become more prominent, however, in source sinks to the present-day southwest of the Appalachian orogens, including the Marathon, Fort Worth, and Arkoma basins, where Pan-African/Brasiliano components along the Ouachita thrust belt contribute zircons with age ranges 800-530 Ma (Thomas, 2021). Detrital zircon and paleocurrent analysis of Atokan sandstones in the Arkoma basin show that 800-600 Ma zircons are present in northeastward-deposited beds but

not in westward- and southward-deposited beds; this observation suggests that 800-600 Ma zircons were sourced not from Gondwanan terranes accreted in the Appalachian region for these sandstones, but rather from Gondwanan terranes to the south-southwest, namely the Yucatan and/or Sabine plates (Sharrah, 2006; Thomas, 2021).

Unlike peaks in Middle Paleozoic grains (discussed in the following section), the 601 and 619 Ma peaks in Neoproterozoic ages for the sample from this study do not seem to prove as useful in narrowing down potential sources, as they are found in units in both the Appalachian region as well as along the Ouachita thrust belt. A slightly metamorphosed granite beneath the present-day Chesapeake Bay yielded a U-Pb zircon age of 614 ± 9 Ma, and although they contained low amounts of Neoproterozoic grains, some samples along the Appalachian thrust belt, such as the Sharon Conglomerate and Grundy-Norton interval, contained peaks of 618 Ma and 619 Ma, respectively (Becker, 2005; Thomas, 2017). Samples from the Baldy Unit and the San Marcos Formation adjacent to the Coahuila block have Neoproterozoic peaks at 596 ± 10 Ma and 618 Ma, respectively (Martens, 2009; Thomas, 2019). The overlap between age peaks necessitates consideration of other factors when determining provenance for Neoproterozoic grains in the Cleveland sample, including relative abundance of grains for different basins, εHf values, provenance of grains in other age ranges, and petrographic work indicating sediment dispersal.

Grains with ages 800-500 Ma display εHf values between +8.5 to -27.3 in the Marathon foreland, while grains in this range present in the Appalachian foreland range from +7 to -13 (Thomas, 2017; Thomas, 2019). In the sample from this study, grains in this range had εHf values between +10.6 and -22.9. The presence of these negative values in the Cleveland sample suggests that Neoproterozoic grains for the Cleveland Sandstone may have been derived from peri-Gondwanan terranes to the south of the study area, rather than Gondwanan terranes accreted along the Appalachian region to the northeast.

Abundance of Neoproterozoic grains in the Cleveland sample suggest a source other than the Appalachians, as Appalachian-derived samples generally have very small Neoproterozoic populations. As discussed in the following section, Middle Paleozoic grains seem to be a good match for sources located south of the study area, which may indicate that Neoproterozoic grains were also derived from these sources. Finally, petrographic work in this study as well as Hentz (1992) and Hentz (2011) strongly suggests a west-east sediment dispersal for the Cleveland Sandstone in the western Anadarko basin; if this were to be the case, Appalachian-derived detritus would have a difficult time entering the system and ultimately being deposited within the Cleveland Sandstone.

7.2.6 Middle Paleozoic (490-270 Ma)

Grains in the 490-270 Ma range are represented in both Laurentian and Gondwanan sources and comprised 9% of concordant ages for the one sample analyzed in this study. Despite their relatively low abundance, understanding provenance of grains in this age range has major implications for sediment dispersal of the Cleveland Sandstone, as the initial hypothesis of the study involved identifying Appalachian-derived grains which would fall in this age range. Distinguishing between the two source areas is difficult on the basis of U-Pb ages alone; however, in-depth characterization of Appalachian (Laurentian) detritus age distributions from multiple studies, as well as insights from sandstone petrography and geometry, allow for certain inferences to be made regarding sources for Middle Paleozoic grains in the Cleveland Sandstone.

Laurentian sources for Middle Paleozoic grains include synorogenic Taconic plutons (490-440 Ma), synorogenic Acadian plutons (420-350 Ma), and synorogenic Alleghanian plutons (330-300 Ma) (Thomas, 2004; Becker, 2005; Thomas, 2017; Thomas, 2020). Each have well-constrained emplacement ages as determined through U-Pb and Hf isotopic analysis. Taconic

plutons are interpreted to be the eroded roots of Ordovician volcanic systems active during the Taconic orogeny, and dates from zircons within K-bentonite beds yield ages around 454 Ma (Thomas, 2004). Magmatic arcs along the New York promontory have ages of 485-470 Ma and 454-442 Ma, and arcs along the Virginia promontory and Pennsylvania embayments have zircon ages of 489-470 Ma, 472-441 Ma, and 438-423 Ma (Thomas, 2017). Plutons contemporaneous with the Acadian orogeny, present in the Pennsylvania embayment, have ages of 381-362 Ma (Thomas, 2017). Finally, synorogenic rocks of the Alleghanian orogeny have ages of 330-300 Ma, with volcanic ash beds within Pennsylvanian-age coal beds having U-Pb zircon dates of 316 ± 1 Ma and 311.2 ± 0.7 Ma (Thomas, 2017; Thomas, 2020).

Thomas (2017) provides a sort of "template" for recognition of detrital zircon populations from Appalachian sources. The primary characteristics he lists are: 1) a general lack of grains older than 1500 Ma; 2) a dominance of Grenville-age grains; 3) small amounts of grains from accreted Gondwanan terranes or Iapetan synrift rocks; 4) a strong component of Taconic and Acadian zircons, and; 5) a general lack of Alleghanian-age grains (Thomas, 2017). A composite relative age-probability plot, shown in Figure 14, illustrates this "Appalachian signature." Detrital zircon dates for the seven Mississippian-Permian samples from Thomas (2017), all interpreted as being Appalachian derived, were quantitatively compared to the sample acquired for this project via the Kolmogorov-Smirnoff test; at the 95% confidence level comparing samples with similar population sizes (only excluding one sample, the southern Sharon Conglomerate sample), no Thomas (2017) samples were statistically likely to have derived from the same source as the Cleveland sample from this study (results in Table 1).

Of the 25 grains with U-Pb ages in this range, 11 grains form a strong probability peak at 416 Ma. Potential sources with grains corresponding to the 416 Ma peak have origins throughout peri-Gondwanan terranes. Zircons from the Mountain Pine Ridge Granite in the Maya block (present-day Brazil) yielded U-Pb ages of 418 ± 3.6 Ma and ages for the Bladen Rhyolite

Formation of 406 Ma (Martens, 2009); Martens (2009) also interprets the Macal Formation, a conglomerate feldspathic litharenite with a single age population at 415 Ma, as being sourced from the Bladen Rhyolite, apparently allowing for some error in the calculated age of the Bladen Rhyolite. Sandstones bordering the Coahuila block, such as the San Marcos and La Casita Formations, also contain Middle Paleozoic grains with peaks around 416 Ma (Thomas, 2019). Finally, plutonic basement rocks of the Yucatan block have been dated at ~418 Ma, and zircons around this age are found in sandstones throughout the Marathon, Fort Worth, and Arkoma basins (Gleason, 2007; Thomas, 2021). The strong peak around this age in the sample from this study suggests that Middle Paleozoic grains originated from Gondwanan terranes to the south of the study area rather than from Appalachian sources to the northeast; this is further supported by mapping of the Cleveland Sandstone by previous studies (Hentz, 1992; Hentz, 2011) as well as the petrographic work performed in this study indicating a west-east sediment dispersal. A Kolmogorov-Smirnoff (K-S) test comparing the Cleveland sample from this study and samples from the Marathon basin and around the Coahuila block from Thomas (2019) suggests that Middle Paleozoic zircons in the Cleveland Sandstone in western Oklahoma are statistically likely to have been sourced from Gondwanan accreted terranes located to the south of the study area (results in Table 2). Additionally, no formations interpreted in previous studies as being sourced from the Appalachian region have peaks at 416 Ma, with the exception of one sandstone sampled above the Princess No. 7 Coal in Kentucky which had a minor peak at 417 Ma (Thomas, 2017).

7.3 Cleveland Sandstone Sediment Dispersal

Incorporation of Cleveland Sandstone petrography with new detrital zircon data indicates a west-to-east trending fluvial system that transported sediment likely derived primarily from Gondwanan terranes accreted along the Ouachita-Marathon thrust belt to the south of the study

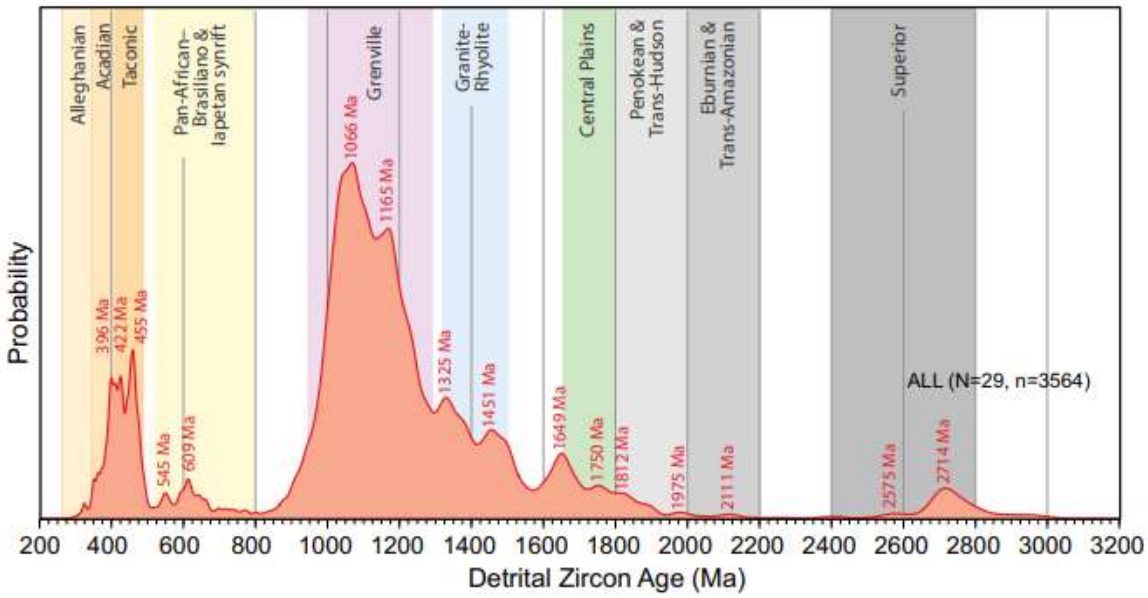

Figure 14. Composite relative age-probability plot of U-Pb analyses reported in Thomas (2017) representing the "Appalachian signature" of detrital zircon populations in the Appalachian foreland. Note the lack of Neoproterozoic grains. From Thomas (2017).

area as well as recycled Grenville-age sediments. The concentration of grains around key Middle Paleozoic and Neoproterozoic peaks allowed for differentiation between Laurentian and Gondwanan sources, as well as comparison of age spectra from the sample analyzed in this study with those from Laurentian-derived (Forest City, Illinois, Appalachian foreland) and Gondwanan-derived (Marathon, Fort Worth, Arkoma) basins. A K-S test statistically showed that the Cleveland sample from this study matched well with samples from Gondwanan-derived basins in terms of provenance, but did not match with samples from Laurentian-derived basins. The lack of grains corresponding to the Wichita uplift (539-530 Ma) and Ancestral Rocky Mountains (1800-1600 Ma) indicate a more distal source for detrital grains within the Cleveland Sandstone. Abundance of Neoproterozoic grains, the presence of strong peaks corresponding to southern Gondwanan sources, and sandstone petrography across the study area suggest that the Appalachians contributed little to no sediment to the western Anadarko basin during Cleveland

deposition. These observations point instead to Gondwanan sources to the south, including the Yucatan, Maya, and Coahuila terranes. A possible secondary source is the Granite-Rhyolite province to the north of the study area; however, grains of this age (1600-1300 Ma) are also present in Gondwanan sources to the south of the study area.

When compared with other Anadarko basin samples (Figure 15) from Thomas (2021), results from this study indicate a rapidly changing sediment dispersal system probably linked to uplift/subsidence of Paleozoic tectonic features and a changing Anadarko basin physiography throughout the Pennsylvanian and Permian. However, samples from Thomas (2021) were located much more proximally to the Wichita and Arbuckle uplifts than was the sample from this study. Nevertheless, the overall lack of detrital zircon data in the western Anadarko basin makes these useful data points and necessitate the comparison described herein.

Stratigraphically above the Cleveland Sandstone, samples from the Virgilian Vanoss Conglomerate all demonstrate an abundance of Superior-age grains, likely indicating recycling from underlying Ordovician rocks, with no Neoproterozoic grains and a very small Middle Paleozoic population (Thomas, 2021). This is clearly a sharp contrast to the age spectra observed in the Cleveland sample, although as previously mentioned this may be more influenced by sample location than true changes in Paleozoic tectonic features and/or basin physiography causing such an abrupt and distinct change; regardless, this observation highlights the spatial and temporal differences in sediment dispersal in the Anadarko basin.

The Post Oak Conglomerate, deposited during the Lower Permian, marks another abrupt change from the underlying Vanoss Conglomerate. Grains from Post Oak Conglomerate samples

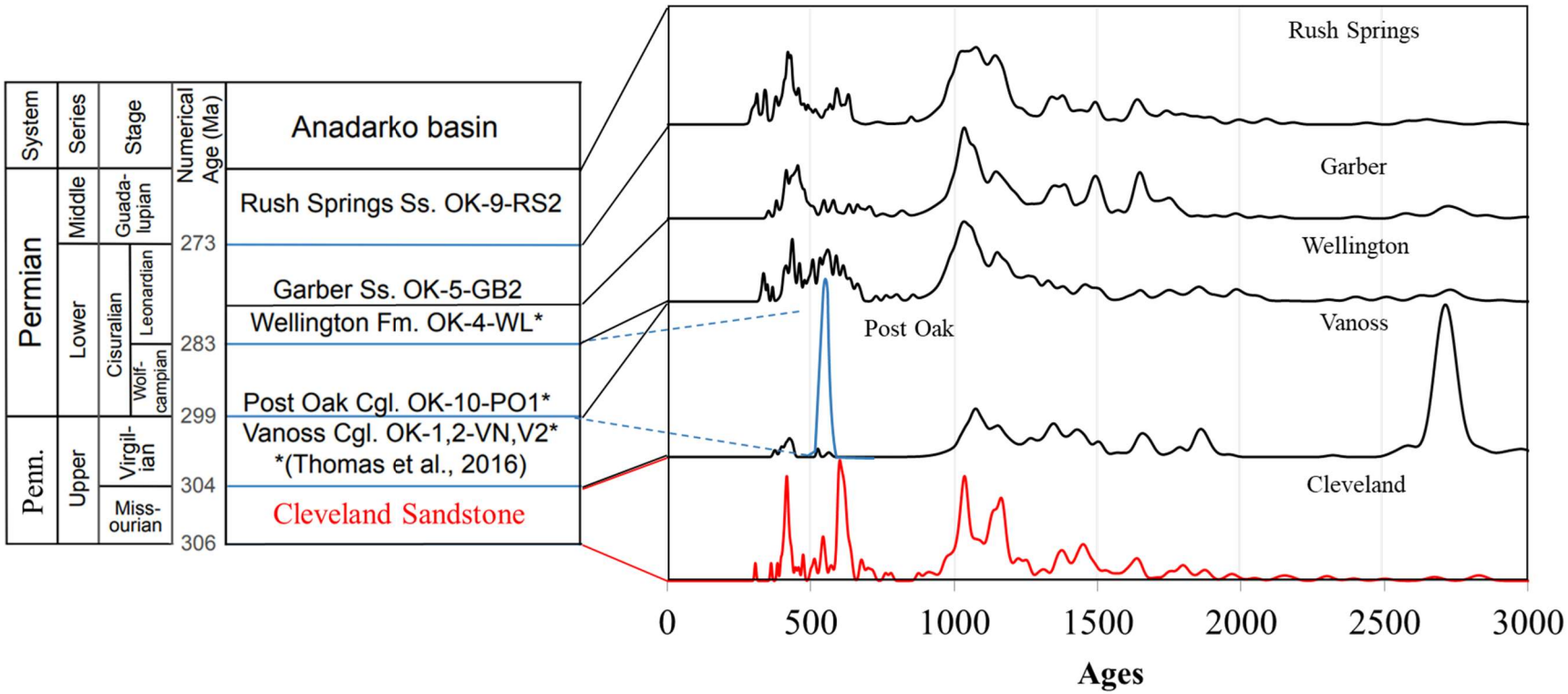

Figure 15. U-Pb detrital zircon age distributions from this study, Thomas (2016), and Thomas (2021) for formations in the Anadarko basin.

in Thomas (2021) belong almost exclusively to the Wichita uplift. By Atokan time, the Wichita uplift had been eroded to its granitic basement and was contributing sediment to the adjacent Anadarko basin (Moore, 1979); the lack of these grains in samples from this project and Thomas (2021) until the Lower Permian, where they suddenly comprise nearly the entire Post Oak Conglomerate, is puzzling. This may indicate that detritus shed from the Wichita uplift was deposited elsewhere prior to deposition of the Post Oak Conglomerate, that the Wichita uplift was periodically inactive during the Late Pennsylvanian, or that sediment dispersal systems had not been developed during the Late Pennsylvanian to transport Wichita-derived detritus to areas where samples were collected.

Following deposition of the Post Oak Conglomerate, later Permian formations in the Anadarko basin indicate more distal sources. The Wellington Formation contains few Superior- and Wichita-age grains, and negative εHf values for Neoproterozoic grains indicate these grains were sourced from Gondwanan sources to the south rather than Cambrian synrift rocks overlapping these ages (Thomas, 2021). Along with the Wellington Formation, the Garber and Rush Spring Sandstones display similar age signatures to formations in the Marathon and Fort Worth basins, containing a significant population of Neoproterozoic grains (Pan-African/Brasiliano) (Thomas, 2021). Both the Garber and Rush Spring Sandstones also contain peaks similar to the Cleveland sample (415 Ma and 420 Ma, respectively).

For the Permian formations in the Anadarko basin interpreted by Thomas (2021) to reflect deposition from the south, sediment transport is thought to occur via deltaic progradation from the Marathon foreland. Transport of these grains via a west-to-east trending fluvial valley in the western Anadarko basin has not been documented and raises further questions on how these grains travel northward until their final deposition. The presence of Gondwanan grains in the Anadarko basin has only recently been discovered by Thomas (2016) and Thomas (2021), however; future detrital zircon analysis of formations in the Anadarko basin should help to further

delineate sediment dispersal from the south and its impact on the distribution of Paleozoic strata. Transport of grains from the south (Figure 16) would involve dispersal through the Ouachita-Marathon depocenters and require crossing the Amarillo-Wichita-Arbuckle uplifts. While this may be difficult via deltaic progradation alone, other possibilities for grain transport exist, such as aeolian and volcanic processes (Thomas, 2021). Additionally, although data from this study suggests a southern source for the sample acquired, it is important to note that plutons located west of the study area, perhaps in New Mexico or the Texas Panhandle regions; lacking detrital zircon data, could be possible sources as well.

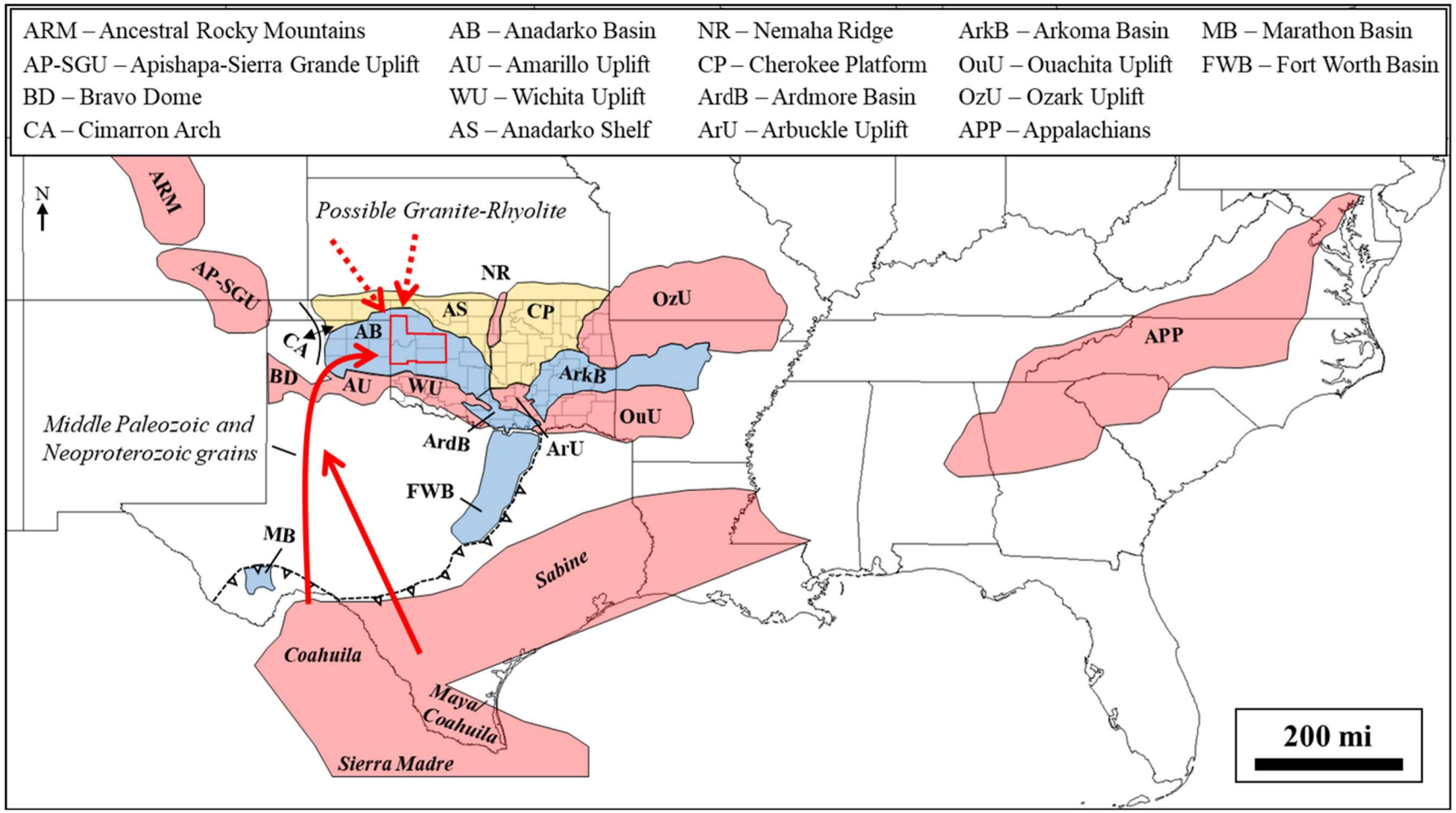

Figure 16. Proposed sediment dispersal for the Cleveland Sandstone in the western Anadarko basin. Compiled from Morris (1974), Moore (1979), Hentz (1992), Becker (2005), Johnson (2008), Miall (2008), and Thomas (2011).

CHAPTER VIII

CONCLUSIONS

In this study, 270 new detrital zircon U-Pb ages and 27 new εHf(t) values were reported for the early Missourian Cleveland Sandstone in the western Anadarko basin. Based on this new data, comparison with coeval strata in multiple basins across the North American Craton, and petrographic work performed in this study, the following conclusions are proposed:

1) Increasing sandstone maturity to the east, as evident by a smaller grain size, better sorting of grains, and a reduction in feldspar content support a west-east trending fluvial system that deposited the Cleveland Sandstone as it occurs in the study area.

2) The change in dominant lithic fragment from metamorphic rock fragments in samples from this study and Hentz (1992) to chert in samples from Bacon (2012) reflects a change in provenance for the formation in north-central Oklahoma to some degree, where local chert-rich sources provide sediment to the Cleveland Sandstone in north-central Oklahoma but not in the western Anadarko basin.

3) The lack of detrital zircon ages corresponding to the Wichita uplift (539-530 Ma) and Ancestral Rocky Mountains (1800-1600 Ma) suggest a more distal extrabasinal source of sediment for the Cleveland Sandstone in the study area.

This may have broader implications for these Late Paleozoic tectonic features, as it may indicate they were not active during Cleveland time, detritus shed from these features were being deposited elsewhere, or sediment dispersal systems had not yet reached the study area.

4) The abundance of Neoproterozoic-age grains and key peaks in Middle Paleozoic-age grains at 416 Ma suggest that these grains were sourced not from the Appalachian region, but rather from sources to the present-day south of the study area in the Yucatan, Maya, and Coahuila terranes. Similarities in detrital zircon age spectra between the sample in this study and samples from coeval strata in the Marathon, Fort Worth, Arkoma, and Anadarko basins, evident through K-S tests performed in this study, further support this conclusion.

5) A potential northern source exists in plutons belonging to the Granite-Rhyolite province; however, overlap of ages with sources to the south means that potentially all grains in the 1600-1300 Ma range were also sourced from these southern sources.

REFERENCES

Algeo, T. J. and P. H. Heckel, 2008, The late Pennsylvanian midcontinent sea of North America: a review, Palaeogeography, Palaeoclimatology, Palaeoecology 268 (2008) 205-221.

Al-Shaieb, Z. and J. W. Shelton, 1981, Migration of hydrocarbons and secondary porosity in sandstones: AAPG Bulletin, v. 65, p. 2433-2436.

Al-Shaieb, Z. et al., 1989, Sandstone reservoirs of the mid-continent, Oklahoma City Geological Society (1989), syllabus for short course.

Bacon, C., 2012, Sequence stratigraphy, reservoir distribution, and diagenesis, Cleveland Sandstone, western Oklahoma, AAPG Bulletin (January 2012) 96 (1): p. 184.

Baker, D. A., 1958, Subsurface geology of southwestern Pawnee County, Oklahoma: University of Oklahoma unpublished M.S. thesis.

Becker, T. P. et al., 2005, Detrital zircon evidence of Laurentian crustal dominance in the lower Pennsylvanian deposits of the Alleghanian clastic wedge in eastern North America, Sedimentary Geology 182 (2005), p. 59-86.

Belt, E. S. et al., 2011, Record of glacial–eustatic sea-level fluctuations in complex middle to late Pennsylvanian facies in the Northern Appalachian Basin and relation to similar events in the Midcontinent basin, Sedimentary Geology 238 (2011) 79-100.

Bennison, A., 1979, Mobile basin and shelf border area in northeast Oklahoma during

Desmoinesian cyclic sedimentation, Pennsylvanian Sandstones of the Midcontinent (1979): p. 283-294.

Bennison, A., 1984, Shelf to trough correlations of late Desmoinesian and early Missourian carbonate banks and related strata, northeast Oklahoma, Limestones of the Midcontinent (1984): p. 93-126.

Cain, C., 2017, Deciphering the Cleveland Sandstone stratigraphic framework: differentiating the Kiefer and Owasso sandstone complexes, north-central and northeastern Oklahoma: Oklahoma State University unpublished M.S. thesis.

Campbell, J. A., 1997, The Cleveland Play: Regional Geology: Oklahoma Geological Survey, Special Publication 97-5, p. 13-29

Carpenter, D. L., 1995, Tectonic history of the Ouachita Interior Zone: New observations from the Sierra Del Carmen, northern Coahuila, Mexico, Gulf Coast Association of Geological Societies Transactions, v. 45, p. 123-126.

Cary, L. W., 1954, The subsurface geology of the Garber area, Garfield County, Oklahoma: Shale Shaker, v. 5, no. 6, p.5-29.

Chapman, A.D. and A. K. Laskowski, 2019, Detrital zircon U-Pb data reveal a Mississippian sediment dispersal network originating in the Appalachian orogen, traversing North America along its southern shelf, and reaching as far as the southwest United States. Lithosphere; 11 (4): 581–587. doi: https://doi.org/10.1130/L1068.1

Clare, P.H., 1963, Petroleum geology of Pawnee County, Oklahoma: Oklahoma Geological Survey Circular 62, p. 62.

Dickinson, W.R. et al., 1983, Provenance of North American Phanerozoic sandstones in relation to tectonic setting: Geological Society of America Bulletin, v. 94, p. 222–235.

Folk, R. L. et al., 1968, Petrology of sedimentary rocks: Hemphills Bookstore, Austin, Texas.

Gehrels, G. E., Johnsson, M. J., & Howell, D. G., 1999, Detrital Zircon Geochronology of the Adams Argillite and Nation River Formation, East-Central Alaska, U.S.A. Journal of Sedimentary Research, 69 (1), 135–144. https://doi.org/10.2110/jsr.69.135

Gehrels, G.E., Valencia, V., & Ruiz, J., 2008, Enhanced precision, accuracy, efficiency, and spatial resolution of U-Pb ages by laser ablation-multicollector-inductively coupled plasma-mass spectrometry: Geochemistry, Geophysics, Geosystems, v. 9, Q03017, doi:10.1029/2007GC001805.

Gehrels, G. E., 2010a, "U-Th-Pb analytical methods." *Arizona LaserChron Center*, 12 August 2010, https://drive.google.com/file/d/0B9ezu34P5h8eMjJiZGZlZTctNDJhNi00NDRlLW IzMmItNzJmMTkwMTIwNTI4/view?resourcekey=0-Z38OEN9DdeufsI2s6IdAAg

Gehrels, G. E., 2010b, "U-Th-Pb analytical methods for zircon." *Arizona LaserChron Center*, 12 August 2010, https://drive.google.com/file/d/0B9ezu34P5h8eMzkyMGFlNjgtMDU0Zi00 MTQyLTliZDMtODU2NGE0MDQ2NGU2/view?resourcekey=0fL7YeK_QPAPRsAlZGZg1Kg

Gehrels, G. E. et al., 2011, Detrital zircon U-Pb geochronology of Paleozoic strata in the Grand Canyon, Arizona: Lithosphere, v. 3, p. 183-200.

Gehrels, G. E. and Pecha, M., 2014a, Detrital zircon U-Pb geochronology and Hf isotope geochemistry of Paleozoic and Triassic passive margin strata of western North America: Geosphere, v. 10 (1), p. 49-65.

Gehrels, G. E., 2014b, Detrital zircon U-Pb geochronology applied to tectonics, Annual Review of Earth and Planetary Sciences, v. 42, p. 127-149.

Gleason, J. D. et al., 2007, Laurentian sources for detrital zircon grains in turbidite and deltaic sandstones of the Pennsylvanian Haymond Formation, Marathon assemblage, west Texas, U.S.A., Journal of Sedimentary Research, v. 77, p. 888-900.

Guynn, J. and G. E. Gehrels, 2006, “Comparison of detrital zircon age distributions using the K-S Test.” *Arizona LaserChron Center*, 25 April, 2006, https://drive.google.com/file/d/0B9ezu34P5h8eZWZmOWUzOTItZDgyZi00NDRiLWI4ZTctNTljNTM5OTU1MGUz/view?amp;hl=en&resourcekey=0-3xtsjeU6TVkRJT2rKg_sHA

Heckel, P. H., 1991, Lost Branch Formation and revision of upper Desmoinesian stratigraphy along Midcontinent Pennsylvanian outcrop belt, Kansas Geological Survey, Geology Series 4.

Hentz, T. F., 1992, Low-permeability, gas-bearing Cleveland Formation (Upper Pennsylvanian), western Anadarko Basin: structure, paleoenvironments, and paleotectonic control of depositional patterns, in Cromwell, D. W., Moussa, M. T., and Mazzulo, L. J., eds., Transactions: American Association of Petroleum Geologists, Southwest Section, Publication No. SWS 92-90, p. 231-252.

Hentz, T. F., 1994, Depositional, structural, and sequence framework of the gas-bearing Cleveland Formations (Upper Pennsylvanian), western Anadarko Basin, Texas Panhandle: The University of Texas at Austin, Bureau of Economic Geology Report of Investigations No. 213.

Hentz, T. F. et al, 2011, Sequence stratigraphy, depositional settings, and production trends of the Middle and Upper Pennsylvanian Cleveland and Marmaton tight-gas sandstones, northwest Anadarko Basin, AAPG Search and Discovery Article #54017.

Hentz, T. F., Ambrose, W. A., and Tussey, L., 2015, Tidal depositional systems in Pennsylvanian strata in the Anadarko Basin, northeast Texas Panhandle, Anadarko Basin, Search and Discovery Article #10742.

“Hf analytical methods at the Arizona LaserChron Center (University of Arizona).” *Arizona LaserChron Center*, https://docs.google.com/document/d/0B9ezu34P5h8eYjhhODFhYTMtNjJiZi00ZWMzLWIwNmQtMjE3NGM1M2EwMzBh/edit?resourcekey=0-T9EFQ0urMVfNMfxZdg9qRg

Hills, J. M., 1963, Late Paleozoic tectonics and mountain ranges, western Texas to southern Colorado: American Association of Petroleum Geologists Bulletin, v. 47, no. 9, p. 1709-1725.

Hoffman, P. F., 1988, United plates of America, the birth of a craton: Early Proterozoic assembly and growth of Laurentia, Annual Review of Earth and Planetary Sciences, 16(1), p. 543-603.

Johnson, K. S., 1989, Geological evolution of the Anadarko Basin, *in* Johnson, K. S., ed., Anadarko Basin symposium, 1988: Oklahoma Geological Survey Circular 90, p. 3-12.

Johnson, K. S., 2008, Geologic history of Oklahoma, Educational Publication 9: 2008, p. 3-8.

Kissock, J. K., Finzel, E. S., Malone, D.H., and Craddock, J.P., 2018, Lower–Middle Pennsylvanian strata in the North American midcontinent record the interplay between erosional unroofing of the Appalachians and eustatic sea-level rise: Geosphere, v. 14, no. 1, p. 141–161, doi:10.1130/ GES01512.1.

Kousparis, D., 1979, Quantitative geophysical study of the Cleveland Sand reservoir (Pennsylvanian) in the eastern part of Logan County, Oklahoma: The Shale Shaker Digest IX, Vol. XXVII-XXIX (1976-1979), p. 92-107.

Kumar, N. and R. Slatt, 1984, Submarine-Fan and Slope Fades of Tonkawa (Missourian-Virgilian) Sandstone in Deep Anadarko Basin, American Association of Petroleum Geologists, v. 68, no. 12, p. 1839-1856.

Lupo, T. and L. Krystinik, 2016, A case study in the Pennsylvanian Cleveland sandstone on the Nemaha Ridge: Leveraging high resolution 3D seismic & stratigraphic analysis to create the conditions for repeatable drilling opportunities in complexly distributed reservoirs, Unconventional Resources Technology Conference (URTeC), #2458016.

Martens, U., Weber, B., and Valencia, V., 2009, U/Pb geochronology of Devonian and older Paleozoic beds in the southeastern Maya block, Central America: Its affinity with peri-Gondwanan terranes, Geological Society of America Bulletin, v. 122, p. 815-829.

McGuire, P.R., 2017, U-Pb detrital zircon signatures of the Ouachita orogenic belt: Unpublished M.S. thesis, Texas Christian University, 43 p.

Miall, A. D., 2008, The sedimentary basins of the United States and Canada, 2008.

Moore, G. E., 1979, Pennsylvanian paleogeography of the southern mid-continent, in Hyne, N. J., ed., Pennsylvanian sandstones of the mid-continent: Tulsa Geological Society Special Publication 1, p. 2-12.

Morris, R. C., 1974, Sedimentary and tectonic history of the Ouachita mountains, Society of Economic Paleontologists and Mineralogists (SEPM) Tectonics and Sedimentation (SP22), 1974.

Pommer, L., et al. 2013, Using structural diagenesis to infer the timing of natural fractures in the Marcellus Shale, AAPG Bulletin (January 2013) 97 (1): 167.

Pullen, A. et al., 2011, "Rock crushing & water table instruction manual." *Arizona LaserChron Center*, 19 February 2011, https://drive.google.com/file/d/0B9ezu34P5h8eYWU3MWMx OWMtMzgxNS00MDNjLTgzYjUtZDU0MmRkYTkxNGMw/view?resourcekey=0-yPhI 9DdbK6_2ItlIMWa0qQ

Rascoe, B., and F. J. Adler, 1983, Permo-Carboniferous hydrocarbon accumulations, mid-continent, U.S.A.: American Association of Petroleum Geologists Bulletin, v. 67, p. 979-1001.

Roddy, C. M. and J. O. Puckette, 2018, Reservoir characterization of the Pennsylvanian Cleveland Sandstone C Unit, Cleveland Field Unit, northeastern Oklahoma, Search and Discovery Article #20438.

Ross, C. A. and Ross, J. R. P., 1987a, Biostratigraphic zonation of late Paleozoic depositional sequences, Geology Faculty Publications 62.

Ross, C. A. and Ross, J. R. P., 1987b, Late Paleozoic sea levels and depositional sequences, Geology Faculty Publications 61.

Rottman, K., 1997, Geology of a Cleveland Sand reservoir, Oklahoma Geological Survey, Special Publication 97-5, p. 30-50.

Scherer, E., Münker, C., and Mezger, K., 2001, Calibration of the Lutetium-Hafnium Clock: Science, v. , p. 683–687.

Schutter, S. R. and P. H. Heckel, 1985, Missourian (early late Pennsylvanian) climate in midcontinent North America, International Journal of Coal Geology, 5 (1985) 111-140.

Sharrah, K. L., 2006, Comparative study of the sedimentology and provenance of the Atoka Formation in the frontal Ouachita thrust belt, Oklahoma (Ph. D. dissertation, University of Oklahoma). Norman, Oklahoma: University of Oklahoma.

Simpson, G. et al., 2012, "Mineral separation instruction manual." *Arizona LaserChron Center*, 1 February 2012, https://drive.google.com/file/d/0B9ezu34P5h8eYzRmZGYwMGItMGI 1MC00MGQ3LWE4YzEtNWZiZmFiNDQ5OGRh/view?resourcekey=0-5BMGpY7CQ1 UwgnbRSYFa9A

Sloss, L. L., 1963, Sequences in the cratonic interior of North America, Geological Society of America Bulletin, v. 74, p. 93-114.

Söderlund, U., Patchett, P.J., Vervoort, J.D., and Isachsen, C.E., 2004, The 176Lu decay constant determined by Lu-Hf and U-Pb isotope systematics of Precambrian mafic intrusions: Earth and Planetary Science Letters, v. 219, p. 311-324.

Stacey, J.S., and Kramers, J.D., 1975, Approximation of terrestrial lead isotope evolution by a two-stage model: Earth and Planetary Science Letters, v. 26, p. 207–221, doi:10.1016/00 12-821X(75)90088-6.

Steiger, R.H. and Jäger, E., 1977, Subcommission on geochronology: convention on the use of decay constants in geo- and cosmochronology: Earth and Planetary Science Letters, v. 36, p. 359-362.

Sundell, K. E., and J. E. Syalor, 2017, Unmixing detrital geochronology age distributions, Geochemistry, Geophysics, Geosystems 18, no. 8: 2872-2886.

Thomas, W. A., 2011, Detrital-zircon geochronology and sedimentary provenance, Lithosphere, v. 3, no. 4, p. 304-308.

Thomas, W. A. et al., 2004, Detrital zircon evidence of a recycled orogenic foreland provenance for Alleghanian clastic-wedge sandstones, Journal of Geology, v. 112, p. 23-37.

Thomas, W.A. et al., 2012, Ages of pre-rift basement and synrift rocks along the conjugate rift and transform margins of the Argentine Precordillera and Laurentia, Geosphere, v. 8, no. 6, p. 1366-1383, doi:10.1130/GES00800.1

Thomas, W. A. et al., 2016, Detrital zircons from crystalline rocks along the Southern Oklahoma fault system, Wichita and Arbuckle Mountains, USA, Geosphere, v. 12, no. 4.

Thomas, W.A., Gehrels, G.E., Lawton, T.F., Satterfield, J.I., Romero, M.C., and Sundell, K.E., 2019, Detrital zircons and sediment dispersal from the Coahuila terrane of northern Mexico into the Marathon foreland of the southern Midcontinent: Geosphere, v. 15, no. 4, p. 1102–1127, https://doi.org/10.1130 /GES02033.1.

Thomas, W. A. et al., 2020, Detrital zircons and sediment dispersal in the eastern midcontinent of North America, Geosphere, v. 6, no. 3, p. 817-843.

Thomas, W. A. et al., 2021, Detrital-zircon analyses, provenance, and late Paleozoic sediment dispersal in the context of tectonic evolution of the Ouachita orogen, Geosphere, v. 17, no. 4, p. 1214-1247.

Triplehorn, D. M., 1965, Origin and Significance of Glauconite in the Geologic Sequence (Abstract), Tulsa Geological Society Digest, Vol. 33, p. 282-283.

Tunin, Z. T., 2020, Detrital Zircon Geochronology and Provenance Analysis of The Desmoinesian (Middle Pennsylvanian) Bartlesville and Red Fork Sandstones, Cherokee Platform and Anadarko Basin, Oklahoma (Master's thesis, Oklahoma State University, 2020). Stillwater, OK: Oklahoma State University.

Turnini, A. M., M. J. Pranter, and K. J. Marfurt, 2019, Mississippian limestone and chert reservoirs, Tonkawa field, north-central Oklahoma, in G. M. Grammer, J. M. Gregg, J. O. Puckette, P. Jaiswal, S. J. Mazzullo, M. J. Pranter, and R. H. Goldstein, eds., Mississippian Reservoirs of the Midcontinent: AAPG Memoir 122, p. 489–512.

Whitmeyer, S. J., and K. E. Karlstrom, 2007, Tectonic model for the Proterozoic growth of North America, Geosphere, v. 3, no. 4, p. 220-259.

APPENDICES

APPENDIX I

Table 1. Results from the Kolmogorov-Smirnoff test comparing the sample from this study with Appalachian samples from Thomas (2017) (Part a are P-values, b are D-values). Yellow highlights indicate > 95% confidence that samples share the same provenance; as discussed above, the Sharon (S) sample value is considered to be erroneous due to the much smaller sample size for the Sharon (S) (Guynn, 2006).

a)

	Cleveland	Stony Gap	Corbin	Sharon (S)	Sharon (N)	Grundy-Norton	Princess No. 7	Proctor SS
Cleveland		0.000	0.000	**0.162***	0.032	0.000	0.000	0.000
Stony Gap	0.000		**0.944**	0.000	0.000	0.000	0.000	0.000
Corbin	0.000	**0.944**		0.000	0.000	0.000	0.000	0.000
Sharon (S)	**0.162***	0.000	0.000		**0.090**	0.000	0.000	0.000
Sharon (N)	0.032	0.000	0.000	**0.090**		0.000	0.003	0.005
Grundy-Norton	0.000	0.000	0.000	0.000	0.000		**0.958**	**0.661**
Princess No. 7	0.000	0.000	0.000	0.000	0.003	**0.958**		**0.971**
Proctor SS	0.000	0.000	0.000	0.000	0.005	**0.661**	**0.971**	

b)

	Cleveland	Stony Gap	Corbin	Sharon (S)	Sharon (N)	Grundy-Norton	Princess No. 7	Proctor SS
Cleveland		0.185	0.206	0.105	0.116	0.238	0.221	0.211
Stony Gap	0.185		0.042	0.257	0.226	0.264	0.223	0.232
Corbin	0.206	0.042		0.265	0.248	0.273	0.236	0.237
Sharon (S)	0.105	0.257	0.265		0.116	0.289	0.251	0.264
Sharon (N)	0.116	0.226	0.248	0.116		0.174	0.148	0.149
Grundy-Norton	0.238	0.264	0.273	0.289	0.174		0.043	0.065
Princess No. 7	0.221	0.223	0.236	0.251	0.148	0.043		0.043
Proctor SS	0.211	0.232	0.237	0.264	0.149	0.065	0.043	

Table 2. Results from the Kolmogorov-Smirnoff test comparing the sample from this study with Marathon basin samples and samples from sandstones proximal to the Coahuila block from Thomas (2019) (Part a are P-values, b are D-values). Yellow highlights indicate > 95% confidence that samples share the same provenance.

a)

	Cleveland	PC04	PC03	PC01	PC02	LR1	TPC2	SM2	PAT1	COALC4	COALC5	TX-14-PGT	TX-12-RC
Cleveland		0.158	0.136	0.145	0.099	0.960	0.575	0.399	0.844	0.927	0.950	0.112	0.211
PC04	0.158		0.061	0.157	0.092	0.835	0.431	0.260	0.710	0.788	0.833	0.222	0.167
PC03	0.136	0.061		0.139	0.090	0.838	0.468	0.287	0.716	0.800	0.832	0.191	0.210
PC01	0.145	0.157	0.139		0.203	0.949	0.567	0.392	0.822	0.903	0.941	0.130	0.225
PC02	0.099	0.092	0.090	0.203		0.877	0.499	0.329	0.753	0.844	0.871	0.192	0.232
LR1	0.960	0.835	0.838	0.949	0.877		0.456	0.643	0.506	0.327	0.166	0.960	0.951
TPC2	0.575	0.431	0.468	0.567	0.499	0.456		0.229	0.315	0.367	0.412	0.629	0.541
SM2	0.399	0.260	0.287	0.392	0.329	0.643	0.229		0.518	0.592	0.637	0.470	0.361
PAT1	0.844	0.710	0.716	0.822	0.753	0.506	0.315	0.518		0.220	0.356	0.852	0.820
COALC4	0.927	0.788	0.800	0.903	0.844	0.327	0.367	0.592	0.220		0.177	0.952	0.903
COALC5	0.950	0.833	0.832	0.941	0.871	0.166	0.412	0.637	0.356	0.177		0.950	0.949
TX-14-PGT	0.112	0.222	0.191	0.130	0.192	0.960	0.629	0.470	0.852	0.952	0.950		0.280
TX-12-RC	0.211	0.167	0.210	0.225	0.232	0.951	0.541	0.361	0.820	0.903	0.949	0.280	

b)

	Cleveland	PC04	PC03	PC01	PC02	LR1	TPC2	SM2	PAT1	COALC4	COALC5	TX-14-PGT	TX-12-RC
Cleveland		**0.177**	**0.330**	**0.262**	**0.721**	0.000	0.000	0.000	0.000	0.000	0.000	**0.541**	0.020
PC04	**0.177**		**0.994**	**0.191**	**0.809**	0.000	0.000	0.003	0.000	0.000	0.000	0.014	**0.118**
PC03	**0.330**	**0.994**		**0.319**	**0.828**	0.000	0.000	0.001	0.000	0.000	0.000	0.049	0.022
PC01	**0.262**	**0.191**	**0.319**		0.039	0.000	0.000	0.000	0.000	0.000	0.000	**0.364**	0.012
PC02	**0.721**	**0.809**	**0.828**	0.039		0.000	0.000	0.000	0.000	0.000	0.000	0.047	0.008
LR1	0.000	0.000	0.000	0.000	0.000		0.000	0.000	0.000	0.000	**0.128**	0.000	0.000
TPC2	0.000	0.000	0.000	0.000	0.000	0.000		0.013	0.000	0.000	0.000	0.000	0.000
SM2	0.000	0.003	0.001	0.000	0.000	0.000	0.013		0.000	0.000	0.000	0.000	0.000
PAT1	0.000	0.000	0.000	0.000	0.000	0.000	0.000	0.000		0.016	0.000	0.000	0.000
COALC4	0.000	0.000	0.000	0.000	0.000	0.000	0.000	0.000	0.016		**0.086**	0.000	0.000
COALC5	0.000	0.000	0.000	0.000	0.000	**0.128**	0.000	0.000	0.000	**0.086**		0.000	0.000
TX-14-PGT	**0.541**	0.014	0.049	**0.364**	0.047	0.000	0.000	0.000	0.000	0.000	0.000		0.000
TX-12-RC	0.020	**0.118**	0.022	0.012	0.008	0.000	0.000	0.000	0.000	0.000	0.000	0.000	

Table 3. XRD and RCA data from Neidens 1-10 core.

SAMPLE DEPTH	8072.5	8088.5	8094.75	8096.5	8103.25	8108.5	8114.1	8116.5	8122	8128	8135	8139	8146	8153	8158.5	8161.25	8167
NON-CLAY FRACTION																	
Quartz	44.9	63.4	65.1	55	62.7	62.2	65.4	42.8	64.2	61.4	63.2	65	62.3	62.9	61.6	61.4	61.2
K-Feldspar	0.7	0.3	0.4	0.5	0.3	0.5	0.4	0.6	0.5	0	0.3	0.5	0.6	0.5	0	0.6	0
Plagioclase	14.3	16.1	16.3	17	18.2	17.5	15.9	10.8	18.6	17.9	18.6	18.4	17.6	18.8	16.7	17.4	16.2
Apatite	0.4	0.3	0.4	0.3	0.3	0.4	0.3	0.5	0	0	0.3	0	0	0	0.6	0.6	0
Pyrite	0.1	0.1	0	0	0	0	0	0	0	0	0	0	0	0	0	0	0
Calcite	16.3	0.5	0.3	0	0.1	0.2	0.5	0.8	0.6	0.1	0.6	2.5	0.1	0	0.6	0.2	2.1
Dolomite	3	0.3	0.7	0.2	0.9	0.6	0.7	22.5	0.6	0.8	0.6	1	1.3	0.9	1.2	0.8	0.5
TOTAL	**79.7**	**81.1**	**83.3**	**73.1**	**82.4**	**81.4**	**83.3**	**78.2**	**84.5**	**80.3**	**83.6**	**87.4**	**81.9**	**83.2**	**80.8**	**81**	**80**
CLAY FRACTION																	
Mixed-Layer Illite/Smectite	2.5	1.9	0.6	1.9	0.9	0.9	2	2.2	0.8	1.7	1.3	0.7	0.9	0.9	0.5	1.8	1.7
Illite + Mica	13.9	12.8	11.8	17.1	13	12.7	11.6	15	10.7	13.6	12	9.3	13.1	11.8	15.4	12.8	13.6
Chlorite	2.9	4.3	4.3	5.8	3.6	4.9	3.1	2.5	4.1	4.3	3.2	2.7	4.1	4.2	3.3	4.4	4.7
Kaolinite	1	0	0	2.1	0	0	0	2.1	0	0	0	0	0	0	0	0	0
TOTAL	**20.3**	**18.9**	**16.7**	**26.9**	**17.6**	**18.6**	**16.7**	**21.8**	**15.5**	**19.7**	**16.4**	**12.6**	**18.1**	**16.8**	**19.2**	**19**	**20**
MEASURED POROSITY	1.8	6.7	9.6	7.6	8.6	9.1	9.1	4.4	9.5	9.6	9.2	9.5	10.2	9.3	8.9	8.5	4.9

Table 4. U-Pb detrital zircon data acquired for the Cleveland sample in this project.

Best age (Ma)	± (Ma)	Conc (%)	Best age (Ma)	± (Ma)	Conc (%)	Best age (Ma)	± (Ma)	Conc (%)
307.7	2.1	121.2	976.0	15.2	99.5	1229.7	11.4	99.4
362.4	2.3	120.6	976.1	12.6	97.9	1244.3	24.9	91.2
384.3	2.2	109.5	990.4	13.1	97.9	1249.8	7.8	98.5
389.5	3.2	85.6	992.8	20.4	102.2	1253.7	10.9	92.3
396.7	2.8	92.7	992.9	15.0	98.7	1255.8	9.6	102.9
403.6	2.2	105.0	995.0	13.6	100.7	1258.3	7.8	100.1
405.0	3.1	101.2	1003.9	23.2	104.6	1289.3	20.3	87.3
407.2	3.1	80.5	1007.6	12.1	102.5	1292.8	10.4	98.0
409.7	2.8	93.2	1011.1	13.0	99.3	1307.4	14.0	95.6
410.7	3.0	107.5	1016.8	12.4	99.6	1308.9	22.0	87.7
413.5	3.4	101.4	1016.9	15.8	98.6	1315.1	8.1	93.4
414.0	2.6	87.0	1018.8	8.0	99.3	1322.0	16.6	80.8
414.7	2.9	97.9	1023.6	11.9	98.9	1323.7	14.0	95.1
414.9	2.5	97.7	1024.4	12.6	104.9	1333.1	30.9	87.9
416.1	2.9	103.3	1024.6	9.5	97.2	1355.5	12.2	101.6
418.7	3.4	105.5	1027.2	11.5	101.0	1356.7	10.6	101.7
418.7	2.7	108.3	1033.2	9.7	99.1	1359.1	9.6	94.6
418.9	2.8	97.2	1033.3	19.6	99.9	1359.7	11.8	101.1
420.5	4.0	114.4	1033.6	10.2	98.8	1360.0	10.5	85.6
421.6	3.0	109.2	1034.2	8.2	98.7	1372.7	9.1	90.7
425.1	2.8	103.4	1034.8	10.5	94.2	1375.3	9.3	102.4
425.4	2.8	79.0	1035.0	16.2	102.0	1377.0	7.8	97.0
427.5	3.1	99.5	1035.2	11.8	101.0	1378.2	8.3	99.6
432.3	2.2	112.0	1037.3	14.2	101.6	1384.1	11.5	95.8
434.5	3.1	107.2	1037.3	9.6	100.5	1386.9	18.2	89.2
439.5	3.1	41.3	1038.2	8.9	97.2	1388.2	8.1	102.1
444.5	3.3	87.6	1039.7	9.1	99.2	1391.3	16.3	81.8
447.8	2.8	110.3	1039.9	7.0	98.9	1394.3	14.8	98.5
458.3	3.0	100.8	1040.0	12.3	97.6	1401.1	10.4	92.3
465.2	2.5	71.9	1040.1	13.1	100.0	1418.3	16.8	97.5
473.9	3.3	101.1	1041.5	9.3	99.9	1421.5	9.5	103.7
474.1	4.1	115.8	1042.0	11.2	99.0	1428.2	8.1	97.5
501.8	3.9	103.3	1043.6	8.2	97.3	1431.8	7.5	96.6
511.5	3.2	130.4	1046.8	11.0	97.6	1436.1	25.6	93.1
515.9	3.7	101.6	1052.1	16.9	100.8	1441.2	10.4	102.3
528.8	11.5	95.4	1052.5	11.9	103.7	1441.9	11.8	101.7

535.1	3.3	99.3	1057.6	8.6	96.6	1445.7	8.2	100.5
542.4	4.2	104.0	1061.1	22.3	91.5	1448.8	10.6	98.6
542.7	4.0	98.6	1061.2	16.7	90.3	1454.8	10.5	99.9
544.3	3.7	97.0	1064.2	7.2	98.4	1455.8	9.0	99.2
545.8	3.9	57.9	1065.1	16.7	102.4	1458.4	12.8	100.6
548.9	6.6	104.3	1069.9	10.8	98.9	1458.7	11.9	97.4
550.9	5.9	75.3	1075.8	9.2	101.3	1460.7	11.6	89.6
552.2	3.1	101.1	1077.9	6.6	92.5	1463.6	7.8	93.1
565.7	6.9	61.6	1078.2	8.5	98.5	1471.1	10.7	101.9
566.0	4.0	71.7	1085.2	6.9	97.4	1483.8	7.8	99.7
567.9	3.5	101.0	1091.2	11.2	100.1	1487.1	7.6	96.6
575.8	5.2	99.9	1093.0	10.1	99.2	1487.6	8.2	92.8
587.0	3.8	96.4	1094.8	10.3	98.0	1492.0	9.6	88.1
593.3	5.4	96.5	1096.8	10.8	95.8	1498.1	11.0	98.2
595.5	3.9	97.5	1100.8	12.5	96.4	1523.7	10.7	93.2
597.7	3.6	90.8	1108.5	9.7	93.1	1525.8	8.3	98.6
598.2	3.2	107.8	1113.2	11.7	97.7	1539.1	7.9	98.1
598.9	3.6	102.7	1114.6	9.6	102.8	1567.1	7.5	98.8
599.7	4.0	92.2	1117.4	11.9	94.7	1568.9	21.1	95.2
600.4	3.2	99.0	1121.2	75.3	93.4	1598.3	15.0	99.7
601.2	4.1	96.9	1121.3	12.0	100.5	1604.3	10.4	99.1
601.7	4.7	111.2	1126.9	8.9	98.9	1620.3	9.0	99.6
602.7	4.3	103.2	1130.1	12.9	100.1	1620.7	7.4	98.2
603.4	3.1	105.2	1130.6	9.6	97.9	1635.3	9.6	97.5
604.5	5.0	95.4	1131.6	11.6	97.2	1638.0	145.8	42.7
606.9	3.9	103.5	1132.4	10.3	104.0	1638.4	11.3	99.6
608.4	4.8	104.7	1132.9	15.6	97.4	1640.9	7.3	95.4
609.7	5.2	119.6	1134.0	13.7	99.1	1643.3	9.4	100.4
609.9	3.2	99.3	1135.6	12.3	98.6	1644.4	7.7	100.0
611.1	4.9	98.8	1136.2	12.1	96.3	1651.7	8.7	98.7
612.0	4.2	112.5	1137.2	11.3	104.6	1701.2	8.4	96.6
612.8	5.0	94.3	1138.8	10.7	99.7	1745.4	8.0	97.6
613.9	4.6	102.0	1143.5	9.3	98.4	1754.6	6.9	98.2
618.1	6.0	104.0	1147.3	13.0	99.1	1755.3	9.2	98.6
618.4	4.0	100.0	1147.4	10.3	99.2	1768.2	7.6	89.1
619.3	3.6	97.4	1149.8	8.9	99.3	1789.0	7.7	99.7
619.9	3.9	95.7	1154.3	13.5	91.3	1797.6	9.2	97.7
620.8	4.0	104.3	1156.6	9.1	96.9	1798.1	8.1	98.5
620.9	4.1	104.0	1157.4	9.8	101.8	1798.4	9.3	98.2
622.9	5.8	63.8	1158.3	12.0	102.5	1805.8	7.7	98.9
624.2	3.0	99.7	1159.8	12.7	101.3	1813.0	9.5	80.8

626.5	3.7	94.3	1160.8	14.8	101.6	1829.5	10.3	91.8
630.3	7.9	98.8	1164.5	6.4	94.9	1863.1	9.4	99.0
632.1	3.9	99.5	1164.7	11.6	98.3	1870.0	8.7	92.8
637.0	5.0	97.3	1167.0	8.4	99.2	1878.3	12.9	90.6
640.4	4.2	109.9	1167.6	8.8	99.1	1885.0	9.2	98.5
643.3	4.3	102.1	1168.5	9.1	99.8	1961.6	10.2	100.0
675.8	5.9	118.0	1168.6	7.4	94.1	1968.6	33.3	93.5
676.0	5.1	100.5	1168.7	11.0	99.5	1975.7	9.1	101.6
684.1	4.8	103.9	1170.8	15.6	100.7	1998.1	8.9	89.4
685.6	5.9	80.6	1171.0	7.6	98.8	2038.9	13.4	84.1
697.8	5.0	93.6	1172.3	9.2	98.0	2048.5	7.8	98.0
707.8	4.8	104.0	1173.1	12.0	99.6	2131.5	10.1	94.4
718.6	5.7	100.7	1174.1	7.6	88.8	2152.3	7.5	93.2
761.9	5.0	103.3	1177.9	11.5	98.4	2177.7	9.0	101.1
780.2	4.9	97.8	1180.1	12.4	99.9	2297.2	9.5	99.5
875.5	5.4	102.4	1189.3	8.2	98.1	2301.4	7.0	96.2
906.0	12.3	100.2	1191.5	12.7	100.4	2392.6	7.1	95.3
907.9	21.1	101.9	1196.2	17.1	90.6	2501.2	7.0	99.9
927.0	13.2	103.0	1211.8	12.4	96.2	2664.3	8.9	99.0
963.0	16.2	98.3	1217.4	12.3	98.3	2684.2	6.3	94.7
966.8	34.2	96.6	1223.9	9.9	95.4	2735.6	173.2	24.8
967.1	10.1	99.6	1229.3	7.9	98.8	2817.6	6.9	99.9
						2832.1	5.5	93.2
						2836.5	8.7	97.0

Table 5. Hf detrital zircon data acquired for the Cleveland sample in this project.

Age	**εHf**
410.6641	-5.41982
707.7977	-9.39635
1431.828	4.884658
619.318	10.56537
420.5491	-2.68945
447.8296	-4.68847
1483.834	5.198808
1064.177	2.549825
601.7357	3.133896
1455.813	-0.00405
626.4504	-18.8929
1359.117	4.9335
1377.008	8.275875
1315.105	3.230598
1788.974	2.103036
1644.431	-2.25123
598.1641	-22.9011
1620.662	2.451384
1164.48	4.297047
1034.241	4.324994
567.9143	8.661931
548.8843	1.05341
414.9377	3.551989
611.9716	-0.1936
362.4313	-12.2425
1043.644	9.289607
1174.14	-23.897

Table 6. Summary of well data acquired for this study. Asterisks (*) indicate wells where point counting was performed.

Name	API	Lat	Long	Desc
RLB	3504323722	36.0706683	-99.2051081	Cuttings, one TS
Smith-Barnes	3504300043	35.9766144	-99.1621987	Photomicrographs, rock mechanics, RCA, XRD, petrologic report, full log suite
Filon Mason*	3504520729	36.2347814	-99.8194884	Photomicrographs, physical TS's, RCA, XRD, full log suite
Mapco Schoenhals*	3504520805	36.2827886	-99.9326209	Core chips, photomicrographs, RCA, XRD
Santa Fe Woodard	3504520963	36.1971731	-99.706013	Photomicrographs, rock mechanics, RCA, XRD, petrologic report, porosity, oil saturation
Braun Guy	3504520974	36.1935607	-99.7015726	Photomicrographs, RCA, XRD, litholog, SP, res
Jordan Stuart*	3504520995	36.2415181	-99.869592	Photomicrographs, physical TS's, RCA, XRD, gamma ray
Hamilton Parker	3504521001	36.0676015	-99.8164725	Photomicrographs, rock mechanics, RCA, XRD, petrologic report
Pet. Neidens	3504521423	36.2185082	-99.9692497	Photomicrographs, RCA, XRD, core description, full log suite
Filon Kline/Pshigoda*	3504520621	36.1621012	-99.9221819	Physical TS's
Williams	3504522866	36.174581	-99.999781	Physical TS's
Weis	4229534328	36.18531	-100.00471	Physical TS's
Lena	4229534326	36.170703	-100.01578	Physical TS's
Coble 1	4223333550	35.9653237	-101.1683987	Physical TS's
Coble 1-24	4223333549	35.9652765	-101.1542094	Physical TS's
Virginia	4235733699	36.288803	-100.800296	Physical TS's
Schultz G	4229533571	36.2472987	-100.2049305	Physical TS's
Schultz	4229532871	36.2663967	-100.1789478	Physical TS's

APPENDIX II – CORE and OUTCROP IMAGES

(Figures 17 – 19)

LITHOTYPE	**CORE (NEIDENS 1-10)**	**OUTCROP (CAIN, 2014)**
Rounded clay pebble conglomeratic sandstone		
Ripple laminated sandstone		

LITHOTYPE	CORE (NEIDENS 1-10)	OUTCROP (CAIN, 2014)
Cross-laminated sandstone		
Massively bedded sandstone		
Interbedded sandstone and shale		

LITHOTYPE	CORE (NEIDENS 1-10)	OUTCROP (CAIN, 2014)
Horizontally laminated sandstone		

Figure 17. Core photographs from the Neidens 1-10 and corresponding outcrop photographs from Cain (2017).

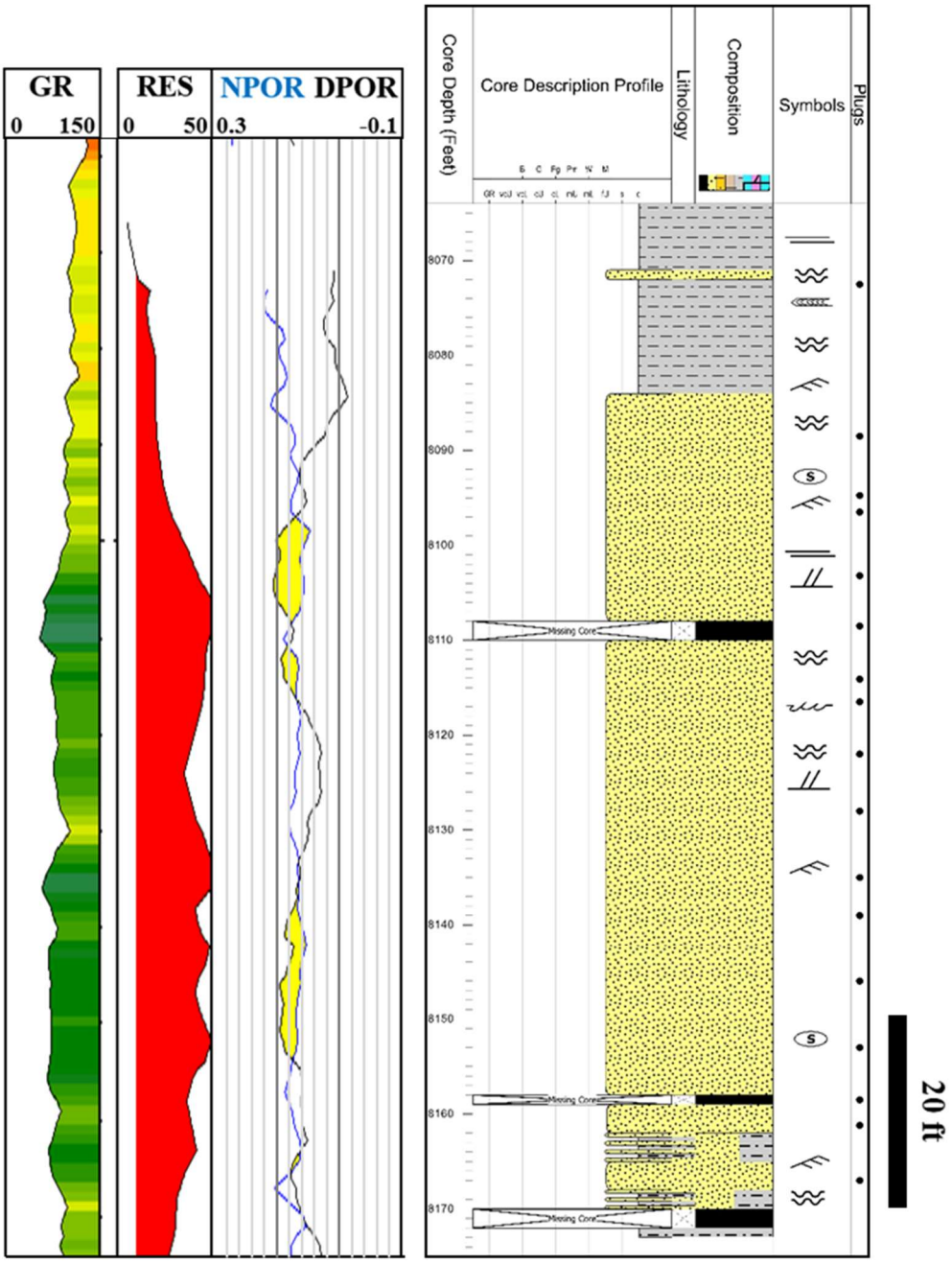

Figure 18. Well logs and core description of Neidens 1-10 core in this study.

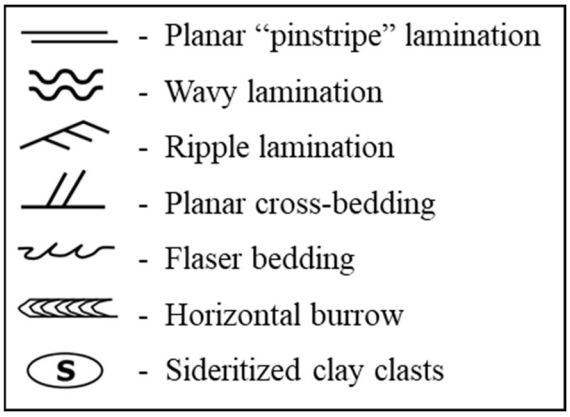

Figure 19. Legend for sedimentary structures in Figure 18.

APPENDIX III – THIN SECTION PHOTOMCIROGRAPHS

Figures 20 - 27

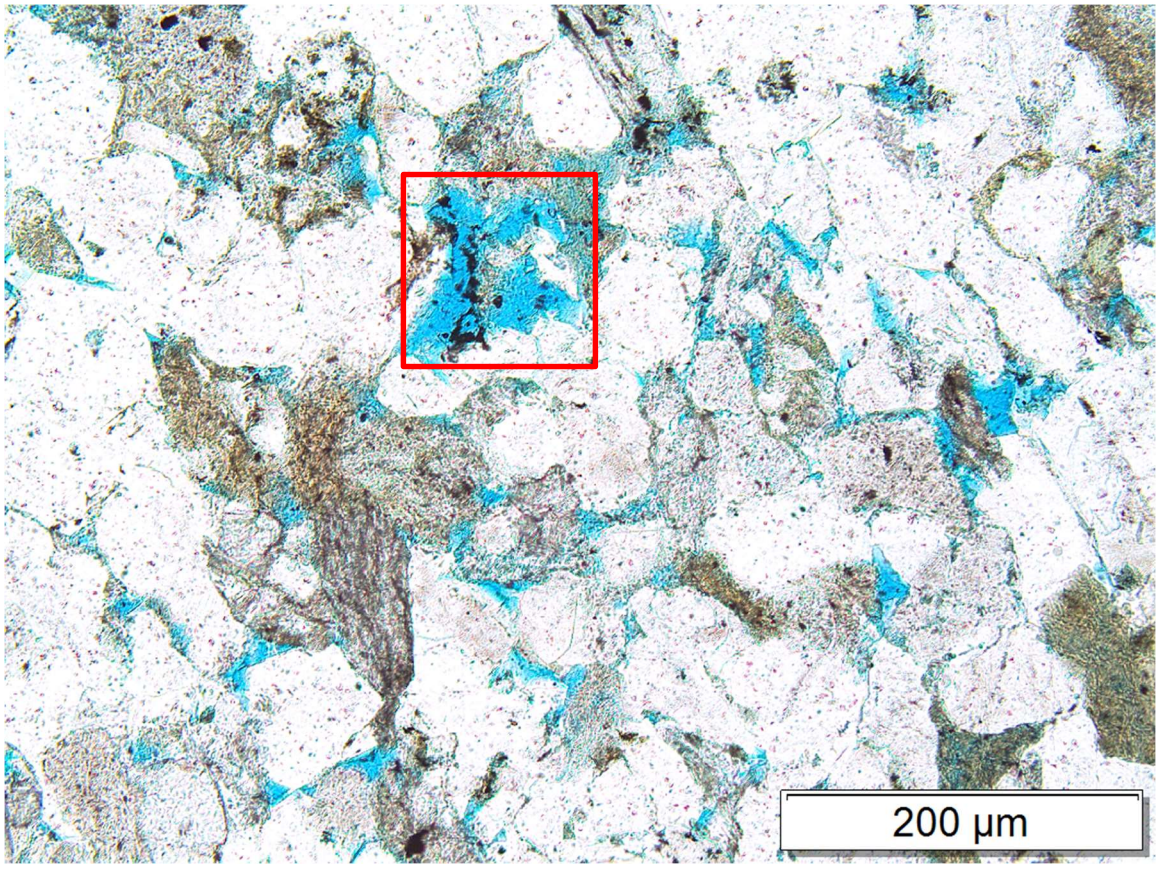

Figure 20. Occurrence of late-stage clay in moldic secondary porosity. Plane-polarized light at 10x magnification in sample FK8377.

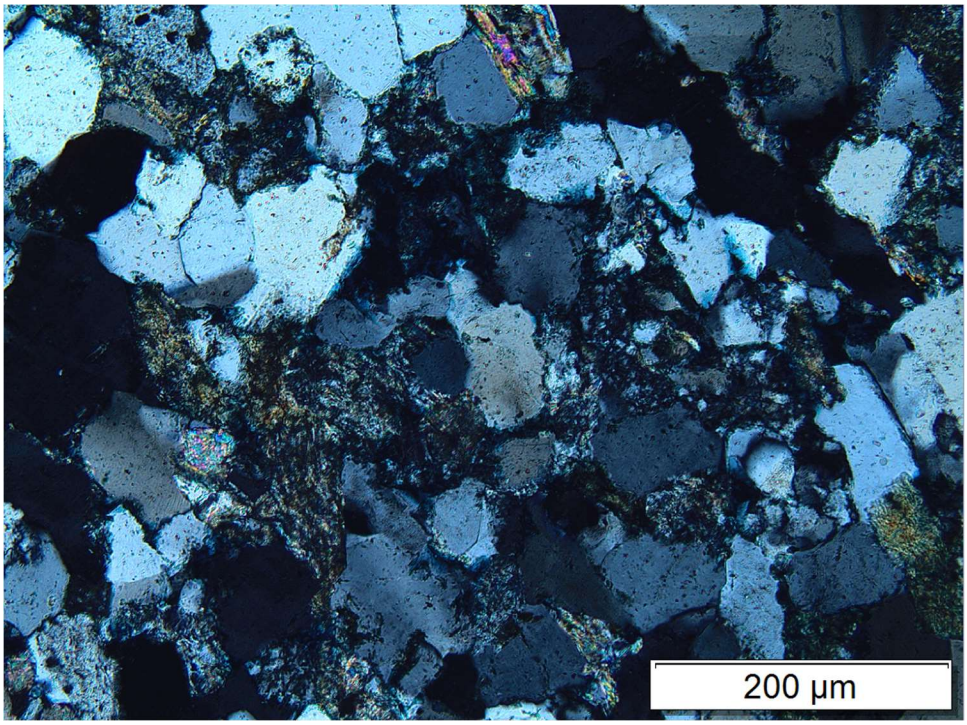

Figure 21. Figure 20 in cross-polarized light at 10x magnification.

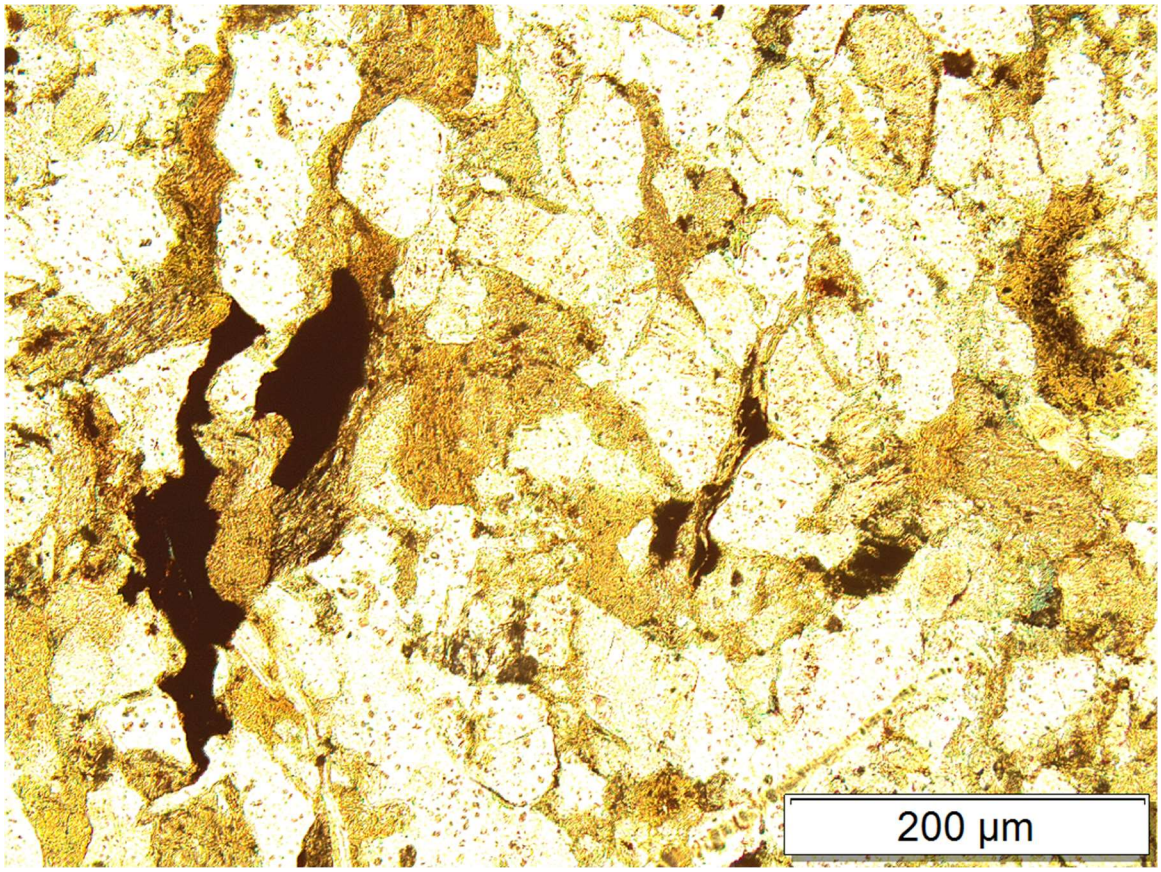

Figure 22. Extensive quartz overgrowths, pseudomatrix from metamorphic rock fragments, and clay occluding porosity. Plane-polarized light at 10x magnification in sample FM8063. Note: thin section likely cut thicker than others, contributing to “yellow” appearance.

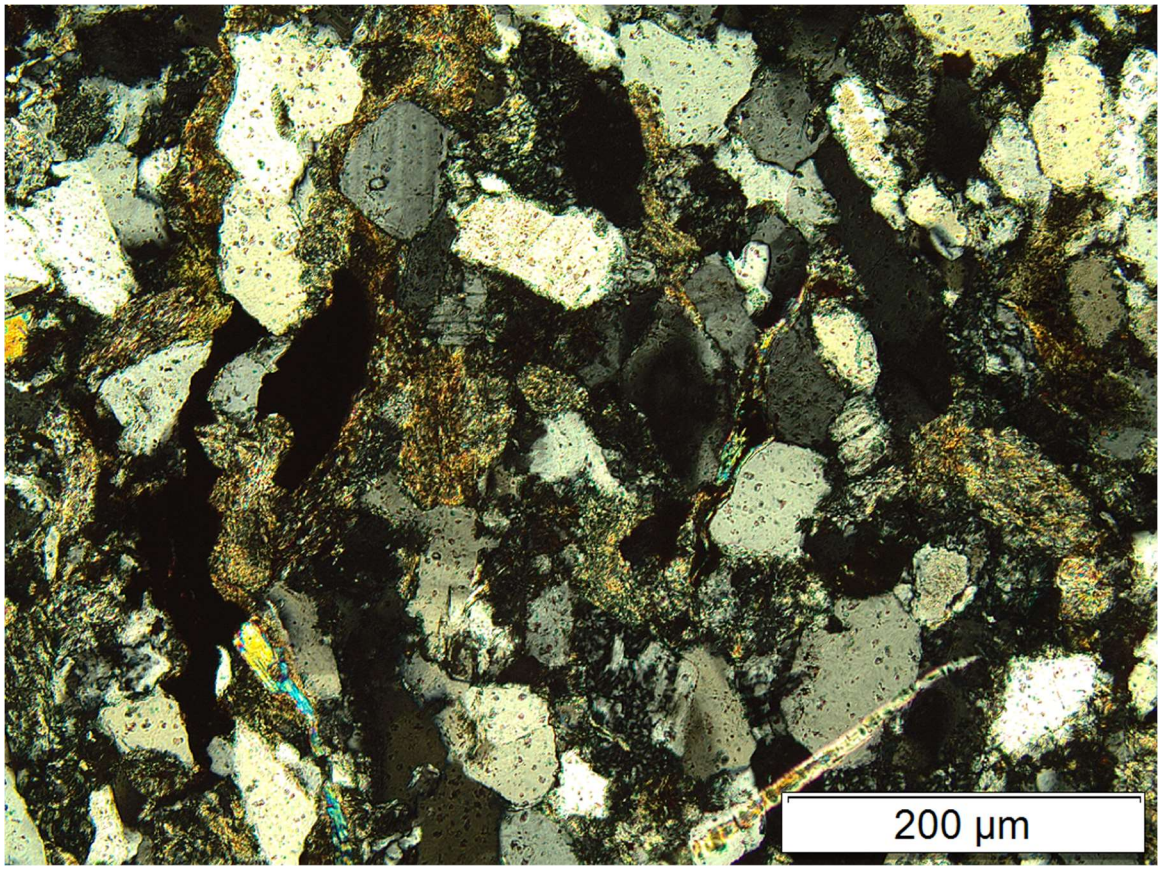

Figure 23. Figure 22 in cross-polarized light. Note mica fragments and abundant metamorphic rock fragments.

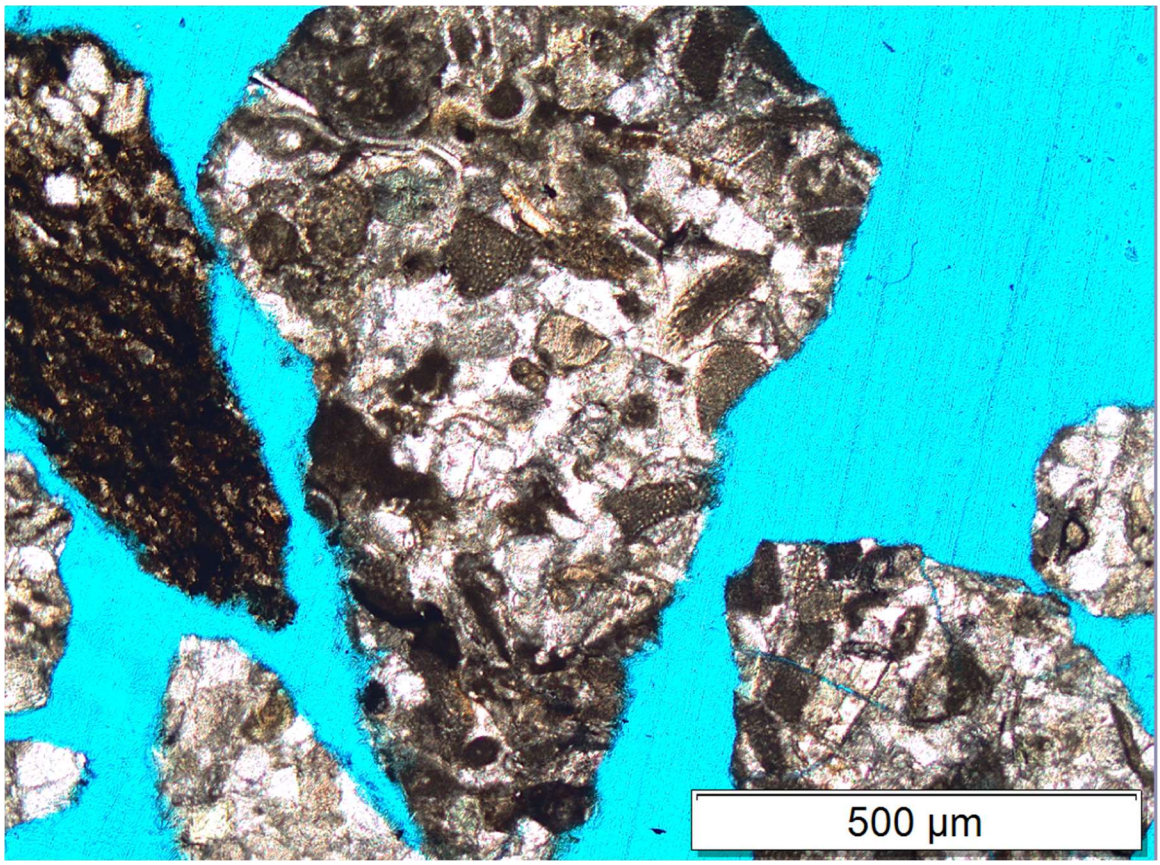

Figure 24. Odd carbonate rock fragments found in cuttings from the Virginia well in the Texas Panhandle. Plane-polarized light at 5x magnification. As noted in the text, this may represent recycling of material from carbonate units stratigraphically adjacent to the Cleveland Sandstone.

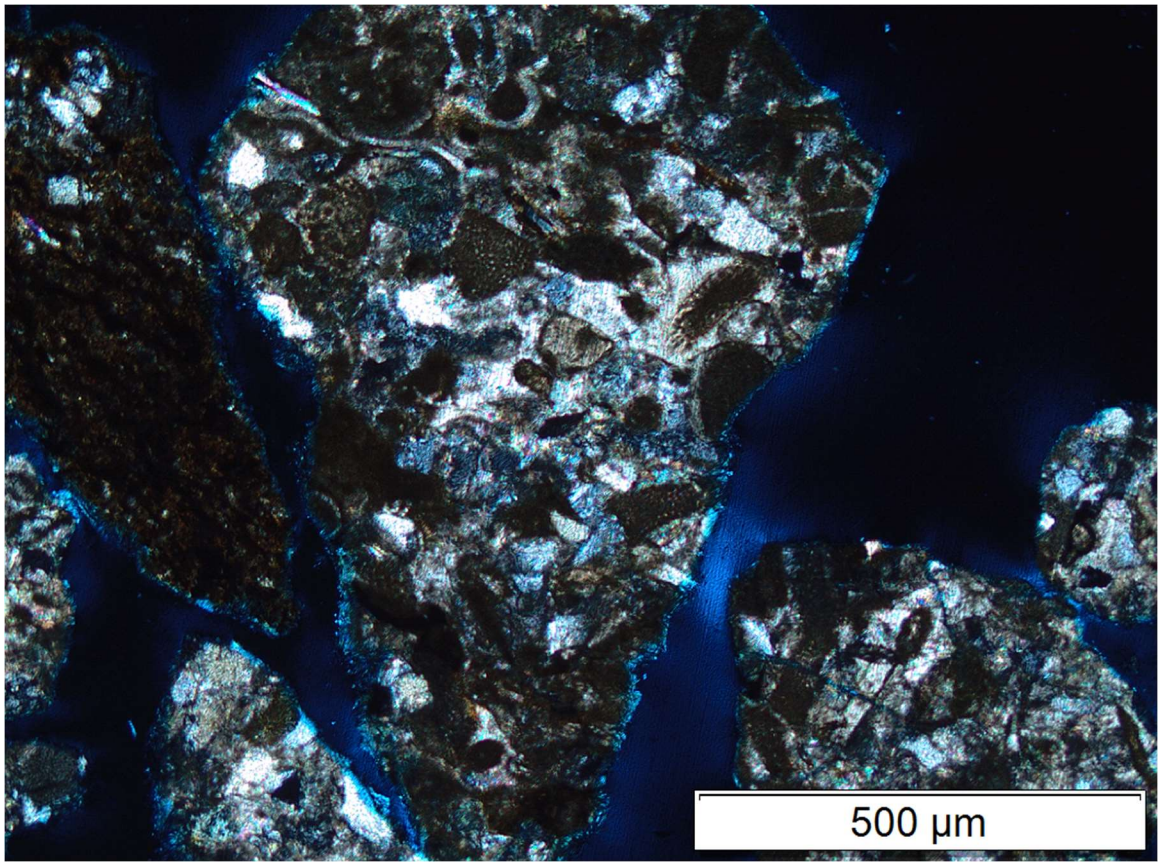

Figure 25. Figure 24 in cross-polarized light.

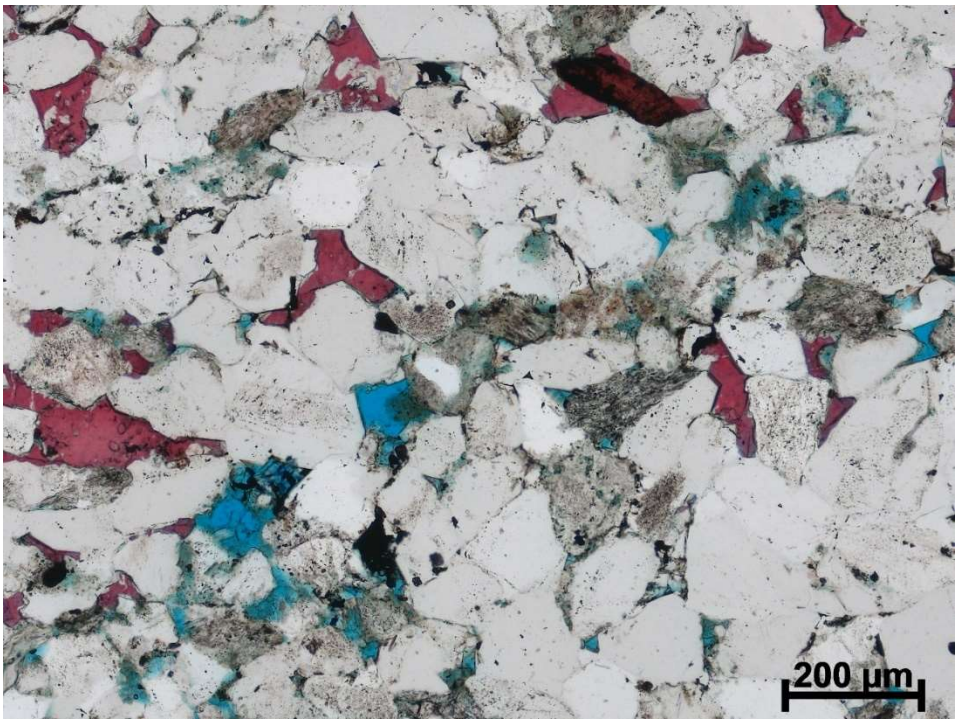

Figure 26. Photomicrograph of the Humble-Smith Barnes well (depth - 8,942') in Dewey County, Oklahoma. Unlike samples from this study, calcite cement was common in photomicrographs from this well. Plane-polarized light at 10x magnification.

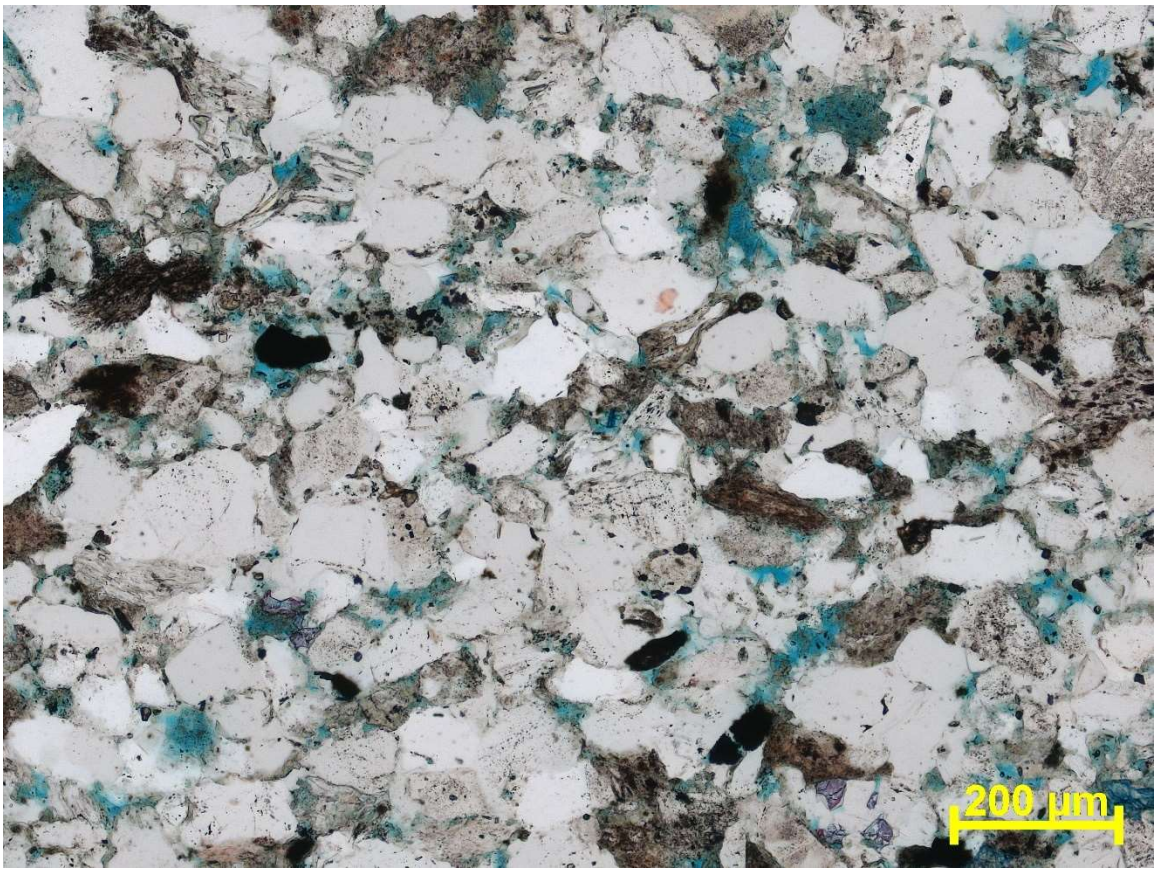

Figure 27. Photomicrograph of the Humble-Smith Barnes well (depth - 9,027') in Dewey County, Oklahoma. As discussed in the text, samples in Dewey County tended to show a reduction in quartz grain size along with better sorting as displayed in this photomicrograph. Plane-polarized light at 10x magnification.

VITA

Brandon M. Weaver

Candidate for the Degree of

Master of Science

Thesis: SEDIMENT DISPERSAL, RESERVOIR QUALITY, AND PROVENANCE ANALYSIS OF THE EARLY MISSOURIAN CLEVELAND SANDSTONE, WESTERN ANADARKO BASIN, OKLAHOMA

Major Field: Geology

Biographical:

Education:

Completed the requirements for the Master of Science in Geology at Oklahoma State University, Stillwater, Oklahoma in May, 2022.

Completed the requirements for the Bachelor of Science in Geology at Texas Christian University, Fort Worth, Texas in 2020.

Experience:

Graduate Research Assistant - Boone Pickens School of Geology, Stillwater, Oklahoma, August 2020 to May 2022
Geology Intern - EOG Resources, Corpus Christi, Texas, Summer 2021
Geology Intern - EOG Resources, Artesia, New Mexico, Summer 2020

Professional Memberships:

Geological Society of America (GSA)
American Association of Petroleum Geologists (AAPG)
Fort Worth Geological Society (FWGS)